



The sphingosine 1-phosphate analogue, FTY720, modulates the lipidomic signature of the mouse hippocampus

Daniela M. Magalhães^{1,2,3}  | Nicolas A. Stewart³ | Myrthe Mampay³ | Sara O. Rolle⁴ | Chloe M. Hall^{3,5} | Emad Moendarbary^{5,6} | Melanie S. Flint³ | Ana M. Sebastião^{1,2} | Cláudia A. Valente^{1,2} | Marcus K. Dymond³ | Graham K. Sheridan⁷ 

¹Instituto de Farmacologia e Neurociências, Faculdade de Medicina, Universidade de Lisboa, Lisboa, Portugal

²Instituto de Medicina Molecular João Lobo Antunes, Lisboa, Portugal

³School of Applied Sciences, University of Brighton, Brighton, UK

⁴Green Templeton College, University of Oxford, Oxford, UK

⁵Department of Mechanical Engineering, University College London, London, UK

⁶199 Biotechnologies Ltd, London, UK

⁷School of Life Sciences, University of Nottingham, Nottingham, UK

Correspondence

Graham K. Sheridan, School of Life Sciences, University of Nottingham, Nottingham, UK.
Email: graham.sheridan@nottingham.ac.uk

Funding information

Fundação para a Ciência e a Tecnologia, Grant/Award Number: PD/BD/128405/2017; The Leverhulme Trust, Grant/Award Number: RPG-2018-443

Abstract

The small-molecule drug, FTY720 (fingolimod), is a synthetic sphingosine 1-phosphate (S1P) analogue currently used to treat relapsing–remitting multiple sclerosis in both adults and children. FTY720 can cross the blood–brain barrier (BBB) and, over time, accumulate in lipid-rich areas of the central nervous system (CNS) by incorporating into phospholipid membranes. FTY720 has been shown to enhance cell membrane fluidity, which can modulate the functions of glial cells and neuronal populations involved in regulating behaviour. Moreover, direct modulation of S1P receptor-mediated lipid signalling by FTY720 can impact homeostatic CNS physiology, including neurotransmitter release probability, the biophysical properties of synaptic membranes, ion channel and transmembrane receptor kinetics, and synaptic plasticity mechanisms. The aim of this study was to investigate how chronic FTY720 treatment alters the lipid composition of CNS tissue in adolescent mice at a key stage of brain maturation. We focused on the hippocampus, a brain region known to be important for learning, memory, and the processing of sensory and emotional stimuli. Using mass spectrometry-based lipidomics, we discovered that FTY720 increases the fatty acid chain length of hydroxy-phosphatidylcholine (PCOH) lipids in the mouse hippocampus. It also decreases PCOH monounsaturated fatty acids (MUFAs) and increases PCOH polyunsaturated fatty acids (PUFAs). A total of 99 lipid species were up-regulated in the mouse hippocampus following 3 weeks of oral FTY720 exposure, whereas only 3 lipid species were down-regulated. FTY720 also modulated anxiety-like behaviours in

Abbreviations: ABC, ATP-binding cassette; AGC, automatic gain control; ANOVA, analysis of variance; APP, amyloid precursor protein; AT, 1-acylglycerol-3-phosphate O-acyltransferase; BBB, blood–brain barrier; CCH, chronic cerebral hypoperfusion; CDase, ceramidase; CDP-DAG, cytidine diphosphate diacylglycerol; CE, cholesteryl ester; CER, ceramide; CerS, ceramide synthase; CNS, central nervous system; CSF, cerebrospinal fluid; CXCL5, LIX chemokine; DG, diacylglycerol; DGAT, diacylglycerol O-acyltransferase; EAE, experimental autoimmune encephalomyelitis; FA, fatty acid; FDA, Food and Drug Administration; FWHM, full width at half maximum; FST, forced swim test; FTY720-P, FTY720-phosphate; HCD, higher-energy collisional dissociation; HESI, heated electrospray ionisation; HPLC-MS, high-performance liquid chromatography–mass spectrometry; LPS, lipopolysaccharide; LTP, long-term potentiation; LysoPC, lysophosphatidylcholine; LysoPE, lysophosphatidylethanolamine; MS, multiple sclerosis; MUFAs, monounsaturated fatty acids; MWM, Morris water maze; OFT, open field test; OPLS-DA, orthogonal partial least squares discriminant analysis; PA, phosphatidic acid; PC, phosphatidylcholine; PCOH, hydroxy-phosphatidylcholine; PE, phosphatidylethanolamine; PEOH, hydroxy-phosphatidylethanolamine; PG, phosphatidylglycerol; PI, phosphatidylinositol; PIP, phosphatidylinositol phosphate; PLA, phospholipase A; PLA2, phospholipase A2; PLC, phospholipase C; PLD, phospholipase D; PND, postnatal day; PPAP, phosphatidic acid phosphatase; PS, phosphatidylserine; PUFAs, polyunsaturated fatty acids; ROS, reactive oxygen species; RT, retention time; S1P, sphingosine 1-phosphate; SM, sphingomyelin; SMase, sphingomyelinase; SPH, sphingosine; SphK, sphingosine kinase; SPP, sphingosine 1-phosphate phosphatase; TG, triacylglycerol.

This is an open access article under the terms of the [Creative Commons Attribution](https://creativecommons.org/licenses/by/4.0/) License, which permits use, distribution and reproduction in any medium, provided the original work is properly cited.

© 2024 The Authors. *Journal of Neurochemistry* published by John Wiley & Sons Ltd on behalf of International Society for Neurochemistry.

young mice but did not affect spatial learning or memory formation. Our study presents a comprehensive overview of the lipid classes and lipid species that are altered in the hippocampus following chronic FTY720 exposure and provides novel insight into cellular and molecular mechanisms that may underlie the therapeutic or adverse effects of FTY720 in the central nervous system.

KEYWORDS

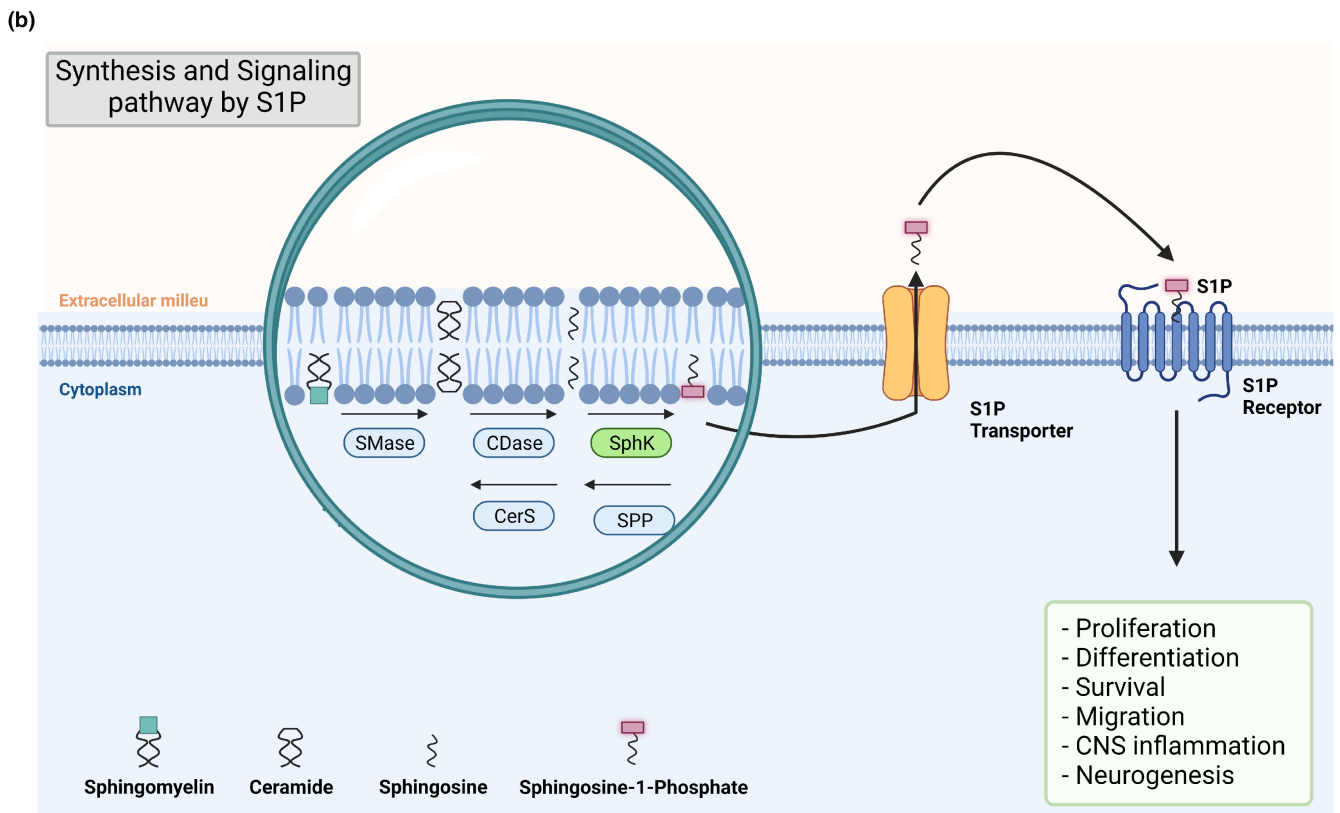
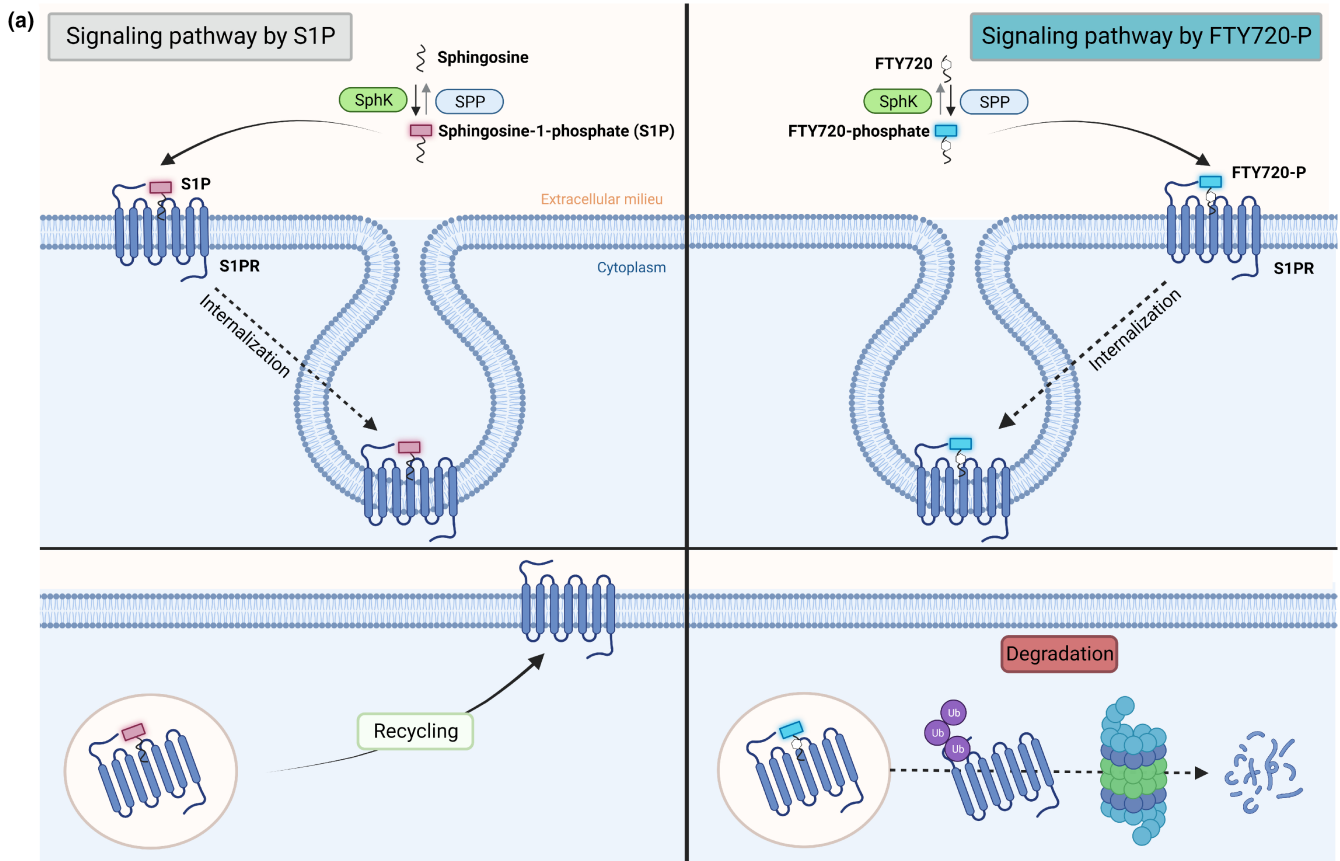
forced swim test, FTY720, hippocampus, lipidomics, sphingomyelin lipids

1 | INTRODUCTION

FTY720, also known as fingolimod, was approved in 2010 by the US Food and Drug Administration (FDA) and became the first oral treatment for relapsing–remitting multiple sclerosis (MS). It is a synthetic compound based on a sphingosine-like fungal metabolite known as ISP-1 (myriocin; 2S-amino-3R,4R-dihydroxy-2-(hydroxymethyl)-14-oxo-6E-eicosenoic acid) and is marketed and sold under the brand name, Gilenya. FTY720 can be phosphorylated *in vivo* by sphingosine kinases (SphKs), producing FTY720-phosphate (FTY720-P; Zemann et al., 2006), which acts as a full agonist on the G protein-coupled sphingosine 1-phosphate (S1P) receptors (S1P1, S1P4, and S1P5) and as a partial agonist at the S1P3 receptor (Dev et al., 2008; O'Sullivan & Dev, 2013). FTY720-P (2-amino-2-[2-(4-octylphenyl)ethyl]-1,3-propanediol monodihydrogen phosphate ester)-mediated activation of S1P1 receptors on endothelial cells can lead to the tightening of cell–cell adhesions in blood vessel walls and inhibition of immune cell trafficking (Sanchez et al., 2003; Wei et al., 2005). FTY720-P also induces internalisation of membrane-bound S1P1 receptors on lymphocytes and targets the receptor for degradation by the ubiquitin proteasome pathway (Figure 1a; Oo et al., 2007), thus inhibiting S1P-mediated chemotactic migration of immune cells from secondary lymphoid tissues. This is thought to be the primary mechanism of action preventing cytotoxic T lymphocytes from crossing the blood–brain barrier (BBB) in MS (Gräler & Goetzl, 2004; Mandala et al., 2002; Matloubian et al., 2004). The non-phosphorylated version of FTY720 has also been shown to inhibit cytosolic phospholipase A2 α in mast cells, independent of S1P receptor activation, which decreases the synthesis of arachidonic acid and eicosanoids in response to bovine serum albumin stimulation (Payne et al., 2007).

In addition to dampening autoimmune responses in MS and inhibiting inflammation, FTY720 can cross the BBB to exert direct effects on cells of the central nervous system (CNS). Autoradiography studies in rats have shown that [14 C]FTY720 is lipophilic and accumulates in the brain and spinal cord parenchyma after a single oral dose (Foster et al., 2007), particularly in white matter areas of the CNS where it can be phosphorylated to FTY720-P by SphK2. Neurons and astrocytes predominantly express S1P1 and S1P3 mRNA transcripts, with lower levels of S1P2 and S1P5 (O'Sullivan & Dev, 2017). Microglial cells express S1P1, S1P2, and S1P3 mRNA transcripts, with little or no S1P5 present (Tham et al., 2003). Oligodendrocytes, on the other hand, mainly express S1P1 and S1P5 receptors (Jaillard et al., 2005; Roggeri et al., 2020). Many of FTY720's therapeutic effects in MS and in other experimental animal models of CNS disease and injury can be attributed to direct activation of S1P receptors (S1P1, S1P3, and S1P5) on neurons and glial cells in different brain regions. For example, FTY720 alleviates mitochondrial dysfunction and reduces microglial-mediated neuroinflammation in the hippocampus of a rat model of chronic cerebral hypoperfusion (CCH; Zhang et al., 2021). FTY720 can also exert positive behavioural effects and attenuate cognitive decline in animal models. For example, FTY720 attenuates spatial memory impairments in the CCH rat model. More recently, it has been reported that chronic oral administration of FTY720 to 3xTg-AD mice, a transgenic animal model of familial Alzheimer's disease, leads to a reduction in neuroinflammation and improvements in both spatial and object recognition memory (Fagan et al., 2022). FTY720-P may exert its effects in the hippocampus, in part, by inhibiting class I histone deacetylases (HDACs), thus enhancing histone acetylation and gene expression programmes important for facilitating learning and memory formation (Hait et al., 2014). FTY720

FIGURE 1 FTY720 and S1P signalling at the S1P1 receptor. (a) Both sphingosine (left panel) and FTY720 (right panel) are phosphorylated via sphingosine kinases (SphKs) and dephosphorylated by sphingosine 1-phosphate phosphatase (SPP). Upon binding to S1P receptors (S1PRs), both sphingosine 1-phosphate (S1P) and phosphorylated FTY720 (FTY720-P) induce internalisation of the receptor. The receptor bound to the S1P lipid is recycled back to the cell surface, whereas FTY720-P leads to receptor ubiquitinylation and proteosomal degradation, thus inhibiting the endogenous sphingosine 1-phosphate pathway. (b) Sphingomyelin at the plasma membrane is transformed into ceramide by sphingomyelinase (SMase). Ceramide can then be converted by ceramidase (CDase) into sphingosine and subsequently into sphingosine 1-phosphate (S1P) by sphingosine kinases (SphKs). The reverse pathway involves S1P dephosphorylation by a specific phosphatase (SPP) to generate sphingosine, which can then be converted into ceramide via the activity of ceramide synthases (CerS). The S1P generated via this so-called 'sphingolipid rheostat' is released into the extracellular space through the action of a specific transporter known as the ATP-binding cassette (ABC) family of transporters. S1P in the extracellular milieu can act in a paracrine or autocrine fashion to bind to S1P receptors (S1P1–S1P5) localised at the plasma membrane of various cell types, consequentially inducing biological responses. Figure created using [BioRender.com](#).



can also modulate the transcription of enzymes involved in ceramide metabolism in the hippocampus of a mouse model of Alzheimer's disease (Ješko et al., 2020).

Ceramide is a metabolite of complex sphingolipids, which are a major component of mammalian cell membranes. Ceramide can act as an intracellular signalling molecule and is also a precursor to sphingosine, an 18-carbon amino alcohol with an unsaturated hydrocarbon chain (Kumari, 2018). Ceramide can be converted into sphingosine through the actions of ceramidase enzymes. In turn, sphingosine can be converted to sphingosine 1-phosphate (S1P) via sphingosine kinases (Figure 1b; Gault et al., 2010; Grassi et al., 2019). During times of cellular oxidative stress, for example, when sphingomyelins in the plasma membrane are broken down to ceramide by sphingomyelinases (SMase) and the levels of ceramide in the cell are high, apoptotic signalling pathways are preferentially activated to initiate programmed cell death. On the other hand, when S1P levels are elevated, cell survival and proliferation signalling programmes are triggered preferentially. Therefore, the balance between cellular concentrations of ceramide and S1P, two interconvertible lipid signalling molecules, is thought to be an important mechanism controlling cell fate and has been termed the 'sphingolipid rheostat' (Cuvillier et al., 1996; Hait et al., 2006).

Lipid signalling in neurons and glia of the CNS is known to be important for many cellular processes including neurotransmission, synaptic plasticity, and axonal myelination (Barber & Raben, 2019; O'Brien & Sampson, 1965; Olsen & Færgeman, 2017; Puchkov & Haucke, 2013). For example, lipids play an important role in neurotransmitter release and synaptic vesicle recycling in neurons (Raben & Barber, 2017). In oligodendrocytes, CNS myelination is dependent on several sphingolipids of the galactosylceramide and sphingomyelin lipid classes (Aureli et al., 2015; O'Brien & Sampson, 1965; Olsen & Færgeman, 2017). FTY720 has been shown to inhibit CNS demyelination (Slowik et al., 2015; Yazdi et al., 2015) and can promote myelin repair following white matter damage (Qin et al., 2017). FTY720 has a 14-carbon chain and possesses cationic surfactant-like properties. In aqueous solution, FTY720 forms small micellar aggregates that can incorporate into phospholipid bilayers and modulate their biophysical properties (Swain et al., 2013). When phosphorylated, FTY720-P crosses the BBB and mimics some of the pharmacological actions of endogenous lipid signalling molecules, such as S1P. As such, FTY720-P most likely possesses the ability to alter the cellular concentrations of certain lipid metabolites and may regulate the molar concentrations of distinct lipid species that comprise the plasma membranes of CNS cell types (Jiménez-Rojo et al., 2014; Swain et al., 2013; Szlasa et al., 2020; Young et al., 2019). Modulation of the physical properties of membranes can impact the functions of transmembrane receptors, and this, in turn, may contribute to the therapeutic actions or to the side-effect profile of drugs such as FTY720.

In this study, we hypothesised that chronic oral dosing of young (adolescent) mice with FTY720 may alter the lipidome of the brain. In 2018, the European Commission approved the use of Gilenya

(FTY720) in children and adolescents, aged 10 years or older, with relapsing–remitting MS. At this age, in both mice and humans, the brain is still undergoing important maturation processes. For instance, axonal myelination of principal neurons continues into adulthood and the proliferation and maturation of interneuron populations, in areas such as the hippocampus, take place during adolescence (postnatal days 21–42) in mice (Le Mageresse & Monyer, 2013; Watson et al., 2006). Therefore, our aim was to investigate the effects of FTY720 on the lipid signature of the maturing hippocampus, a region of the brain important for learning and memory formation (dorsal hippocampus; Fanselow & Dong, 2010; Klur et al., 2009; Moser et al., 1995; Pothuizen et al., 2004), as well as for processing emotional stimuli, regulating mood, and modulating the body's response to stress (ventral hippocampus; Fanselow & Dong, 2010; Ferbinteanu & McDonald, 2001; Henke, 1990; Kjelstrup et al., 2002). The study objectives were twofold: (1) to perform a battery of hippocampal-dependent behaviour tasks in control and drug-treated adolescent mice and to investigate the effects of FTY720 on anxiety and memory formation, and (2) to investigate how FTY720 affects the lipidome of the hippocampus (in behaviour-naïve adolescent mice). Our results suggest that FTY720 causes significant up-regulation of several sphingomyelin lipids (also known as ceramide phosphocholines) in hippocampal cells. We also found a number of other membrane lipids whose concentrations were significantly altered. Thus, our results pave the way for a more complete understanding of the myriad actions of FTY720 on CNS neurons and glial cells, at a key stage in adolescent brain maturation, and the potentially important role of lipid signalling in FTY720's mechanism of action in the central nervous system.

2 | MATERIALS AND METHODS

2.1 | Ethics statement

This study was not pre-registered. All experiments involving animals and schedule 1 protocols used to obtain brain tissue were approved by the Animal Welfare and Ethical Review Body (AWERB committee) of the University of Brighton and carried out under UK Home Office licence-approved protocols. This study was conducted in accordance with the principles of the Basel Declaration and adhered to the legislation detailed in the UK Animals (Scientific Procedures) Act 1986 Amendment Regulations (SI 2012/3039). All efforts were taken to maximise animal welfare conditions and reduce the number of animals used in accordance with the European Communities Council Directive of 20 September 2010 (2010/63/EU).

2.2 | Animals

The study was performed using male C57BL6/J mice (Charles River UK Ltd). No exclusion criteria were pre-determined. All animals were

housed under an artificial 12-h light-dark cycle (07.00–19.00) and controlled room temperature (19–21°C) and humidity (40–60%). Food and water were available *ad libitum*. A total of 30 animals were used in this study, that is, 19 mice (control $n=9$ and FTY720 $n=10$) for lipidomic analysis of hippocampal brain tissue and 11 mice (control $n=6$ and FTY720 $n=5$) for behavioural evaluation. No randomisation was performed to allocate subjects in the study. The mice subjected to behavioural paradigms were different to those used for lipidomic analysis to ensure that the stress associated with behaviour did not impact the hippocampal lipidome in any way. At postnatal day 21, male mice were weaned and separated into either control group or drug treatment group (FTY720). FTY720 was provided *ad libitum* in the drinking water at a concentration of 3.3 µg/mL for 21 days (P21–P42), and the vehicle control group received 0.033% DMSO in their drinking water. Both FTY720 water and DMSO vehicle control water were refreshed once per week (i.e. twice in total) over the course of the 21-day experiment. Several studies have demonstrated the stability of FTY720 at therapeutic concentrations in the drinking water of rodents (Chiba et al., 2011; Kocovski et al., 2021; Metzler et al., 2008; Wang et al., 2014). We have previously shown behavioural effects of oral FTY720 at the same dose in the experimental autoimmune encephalomyelitis mouse model of multiple sclerosis (Sheridan & Dev, 2014). Behavioural evaluation was performed on the final 5 days of drug treatment between 10.00 am and 12.00 noon each day and consisted of the forced swim test (day 38), open field test (day 39), and Morris water maze (days 40–42) to assess despair-like behaviour, anxiety, and spatial memory, respectively. On the last day of drug treatment (P42), mice that had undergone behavioural assessment were weighed and it was noted that the body weight of FTY720-treated mice was, on average, approximately 23% lower than controls (Figure 2a). However, studies have shown that there is a non-proportional relationship between body weight and absolute brain weight in rodents of the same age and sex (Bailey et al., 2004). Therefore, it is very unlikely that there was a 23% decrease in brain weight in the FTY720-treated mice, although we did not weigh brain tissue samples before freezing to ensure that there was only minimal degeneration of hippocampal tissue prior to mass spectrometry analysis. All mice were killed by cervical dislocation followed swiftly by terminal cessation of blood flow via decapitation, and the hippocampus was dissected from the brain, snap frozen in liquid nitrogen, and stored at –80°C until further analysis (Figure 2a).

2.3 | Forced swim test

Before the task began, mice were habituated to the behavioural room in individual cages for 30 min. Each mouse was placed in an individual clear glass cylinder (20 cm in height and 15 cm in diameter) filled with 1.4 L of water at a temperature of $25 \pm 3^\circ\text{C}$ (Figure 2a). The forced swim test lasted 6 min and was recorded with a video camera. Only the last 5 min of the task were studied, since the first minute is considered the habituation phase. Two main behaviours

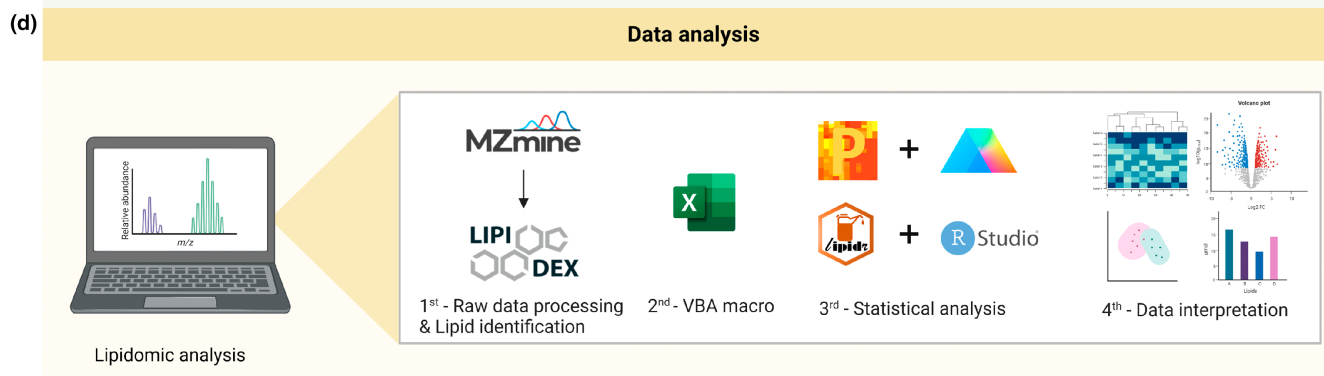
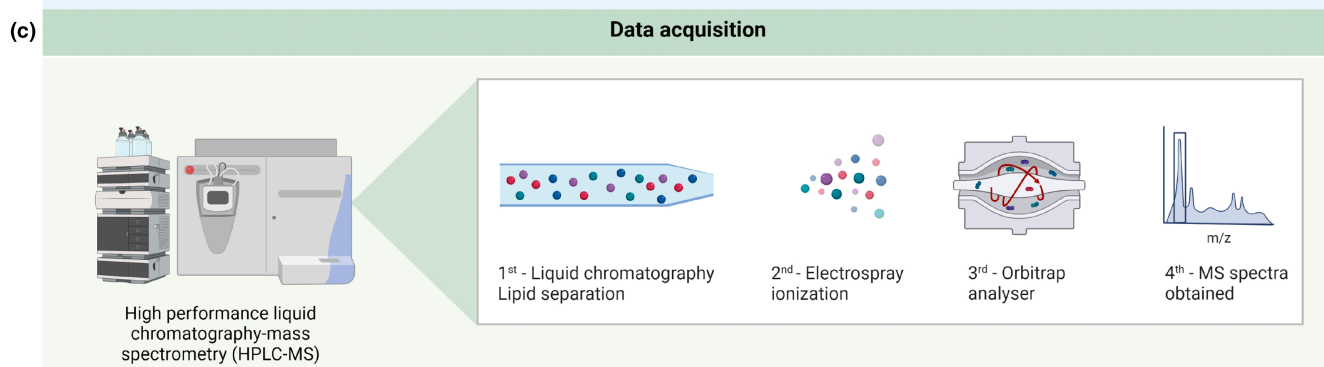
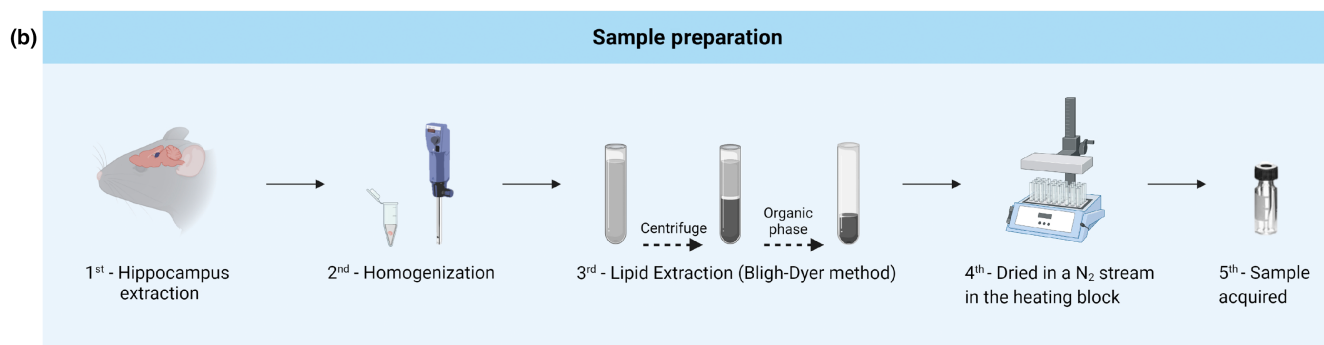
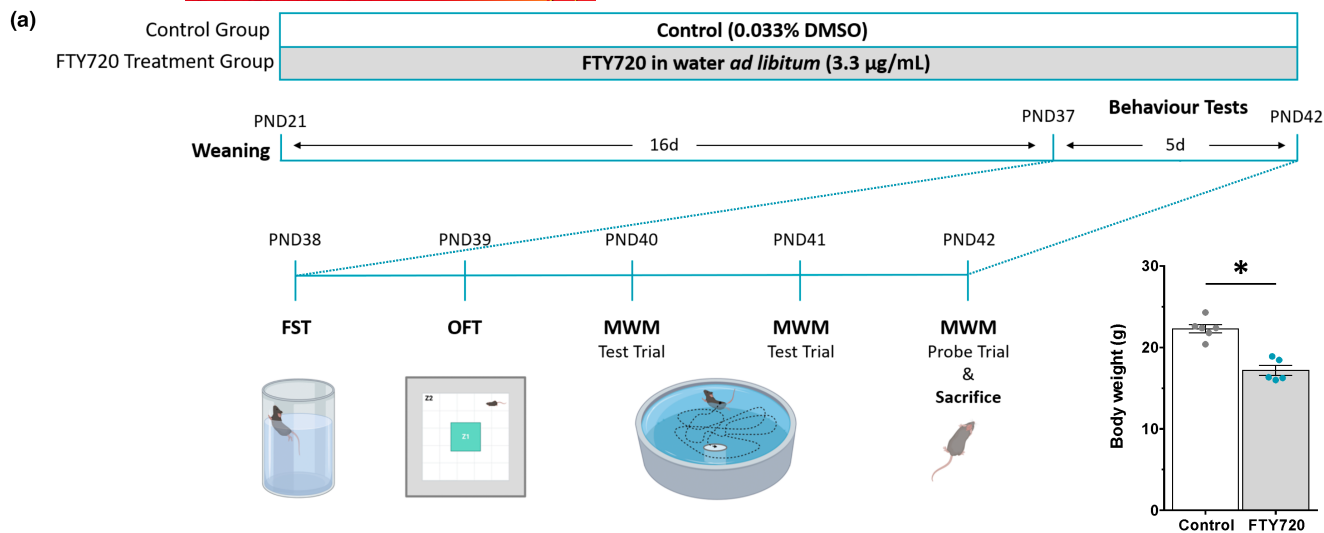
were analysed in order to assess depression-like behaviour in mice (Porsolt et al., 1977), (a) immobility time, defined as minimum whole-body movements with the exception of the necessary movement needed to keep their heads above water, and (b) escape behaviour, described as vigorous climbing movements executed with forepaws above the water level and along the cylinder wall, indicating an attempt to escape. The apparatus was cleaned and filled with fresh water after each use, while each mouse was dried and returned to their home cages. All measurements were manually scored and expressed as percentage values.

2.4 | Open field test

Before the task began, mice were allowed to adapt to the experimental room for 30 min. Mice were then individually placed in the central region of the apparatus and allowed to explore for 10 min, while being videotaped. The apparatus consisted of a white acrylic plastic box (60 × 60 × 30 cm, l × w × h) divided into a central square (zone 1) and the surrounding borders (zone 2; Figure 2a). The apparatus was cleaned with 70% ethanol after each mouse. The ratio of time spent in the outer zone compared to the central zone (Z2:Z1), the distance travelled, and the amount of time each mouse remained immobile were calculated, using ANY-maze software (Stoelting Europe), to assess anxiety-like behaviour (Choleris et al., 2001).

2.5 | Morris water maze

The Morris water maze task was performed to assess spatial learning and memory (Morris, 1981). The water maze apparatus consisted of a circular pool (60 cm diameter and 16 cm height) with water depth of 8.5 cm at a temperature of $25 \pm 3^\circ\text{C}$. For analysis, the pool was divided into four quadrants of equal size. A hidden circular platform (4 cm diameter), constructed from transparent acrylic, was submerged 0.2 cm below the water surface at a distance of 6 cm away from the wall in one of the four quadrants. Surrounding the pool were four different visual cues to help guide the mice to the correct quadrant where the escape platform was located (Figure 2a). Mice were lowered into the water, facing the wall, at one of three possible quadrant starting positions (the platform quadrant was excluded as a starting position), which were randomised in each trial. The spatial learning task consisted of a two-day training period with four trials per animal each day. Each trial lasted a maximum of 90 s, and the escape latency was measured. Mice that successfully found the hidden platform were allowed to remain on it for 30 s for the first trial and for 10 s in the following trials. At the end of each trial, mice were dried-off and returned to their individual trial cages during the inter-trial interval of 15 min. In the case of an incomplete trial (mice that did not locate the platform within 90 s), the mouse was guided to or placed on the platform for 30 s to allow it to orientate itself. At the end of the training session, mice were dried-off and placed back into their home cages. Hippocampal-dependent



spatial reference memory was assessed through a probe trial 24h after the final training session. For the probe trial, the platform was removed and mice were placed into the pool for 60s. The task was

recorded with a video camera, and the percentage of time spent in the platform quadrant was calculated. The videos were analysed offline using ANY-maze software (Stoelting Europe).

FIGURE 2 Schematic representation of the experimental timeline, behavioural tasks, lipidomic workflow, and the data analysis conducted in this study. (a) Post-weaning mice (PND21) were administered FTY720 orally (ad libitum) via the home cage water bottle at a concentration of 3.3 µg/mL or 0.033% DMSO (control mice) throughout the 3-week study protocol. Behavioural tasks were performed during the last 5 days (PND 38–42) of the experiment. Immediately prior to killing, mice were weighed and it was noted that FTY720-treated mice weighed 17.2 ± 1.4 g, whereas control mice weighed 22.3 ± 1.3 g (unpaired Student's *t*-test, $t = 6.435$, $df = 9$, $p = 0.001$). PND, postnatal day; d, day; FST, forced swim test; OFT, open field test; MWM, Morris water maze. (b) Sample preparation involved dissection of the hippocampus from FTY720- or DMSO-treated mice that were not exposed to behavioural task training. The brain tissue was homogenised using standard protocols, and lipid extraction was performed via the Bligh–Dyer method. (c) Data acquisition was performed by high-performance liquid chromatography–mass spectrometry (HPLC-MS) on a hybrid quadrupole Orbitrap mass spectrometer. (d) The first step of the data analysis required the processing of raw values through the MZmine 2 program, followed by lipid identification with the LipiDex software package. A Microsoft Excel macro was created to run the initial lipid species evaluation. Statistical analyses were performed through Perseus software, GraphPad Prism, R Studio, and the lipidr package. Figure created using BioRender.com.

2.6 | Lipid extraction

Mouse hippocampal tissue disruption was performed in 0.9 wt% NaCl (isotonic saline) with a motor-driven tissue homogeniser, followed by the addition of lipid standards in each sample (SPLASH LipidoMIX™ Internal Standard, Avanti Polar Lipids, Alabaster, AL, USA). Total lipid extracts were prepared using a four-step Bligh–Dyer extraction protocol (Bligh & Dyer, 1959). The procedure was as follows: (1) 1.25 volumes of CHCl₃ (chloroform), (2) 2.5 volumes of MeOH, (3) 1.25 volumes of CHCl₃, and (4) extraction was finalised with 1.25 volumes of H₂O. The separation of phases was achieved by centrifugation for 10 min at 4°C. Afterwards, the organic phase (lower phase) was transferred to a glass tube and dried in a N₂ stream in the heating block at 40°C for 30–40 min (Figure 2b). The final step comprised the addition of CHCl₃ and transference to an amber vial (with glass insert).

2.7 | Lipid detection by high-performance liquid chromatography–mass spectrometry

Lipid samples were separated according to previously published methods (Bahja et al., 2022) with an ultra-high-performance LC system (UltiMate 3000, Thermo Scientific) using a reverse-phase ACQUITY UPLC HSS T3 Column (100 Å, 1.8 µm, 2.1 mm × 100 mm, Waters Corporation) set to 40°C. Detection was performed on a hybrid quadrupole Orbitrap mass spectrometer (Q Exactive, Thermo Scientific). The solvent system used was solvent A (60:40 v/v); water (hypergrade for LC-MS, LiChrosolv®, MerckKGaA); acetonitrile (MS suprasolve®, Sigma Aldrich) and 10 mM ammonium formate (99.995%, Sigma Aldrich), and solvent B (90:10 v/v); isopropanol (Optima™ LC/MS Grade, Fisher Scientific); acetonitrile and 10 mM ammonium formate. Solvent flow rate was 200 µL/min, diverted to waste for the first 30 s. The following solvent gradient was used, 100% A (0–1 min), raised to 100% B over 53 min, held at 100% B for 3 min, reduced to 0% B in 1 min, and equilibrated for 9 min. An injection volume of 5 µL was used in µL pick-up injection mode. All samples were stored in the autosampler at 4°C and measured in positive and negative ionisation modes, using heated electrospray ionisation (HESI). Spray voltage was set to 3500 V for positive mode and –3500 V for negative mode, sheath gas was 45 au, auxiliary gas was 8

au, sweep gas was 1 au, and probe temperature was 350°C. Capillary temperature was 320°C, and S-Lens was 50. MS data were acquired in a data-dependent manner, with full scan profile MS spectra (250–1200 *m/z*) recorded at a resolution of 140 000@200 *m/z* followed by the fragmentation of the top 10 most abundant precursor ions. Dynamic exclusion was 10 s, with charge exclusion for unassigned and singly charged species. Automatic gain control (AGC) target was 1×10^6 ; maximum injection time was 50 ms for a full scan. Precursor ion fragmentation was performed by higher-energy collisional dissociation (HCD) using a normalised stepped collision energy of 25 and 30, with a default charge state of 1. MS/MS scans were recorded in profile mode, performed at a resolution of 17 500@200 *m/z* with an AGC target value of 1×10^5 and a maximum injection time of 100 ms using an isolation window of 1.0 *m/z* (Figure 2c).

2.8 | Lipid identification parameters

Lipid identities were assigned using LipiDex software (Hutchins et al., 2018). Spectral searching settings were as follows: MS1 search tolerance (0.01 *m/z*), MS2 search tolerance (0.01 *m/z*), and MS2 low mass cut-off (61.00). Peak finding settings, performed using separate polarity files (produced in MZmine, see below for details), with MS/MS filtering parameter were as follows: min lipid spectral purity (75%), min MS2 search dot product (500), and min MS2 search reverse dot product (700). Feature association parameters were full width at half maximum (FWHM) window multiplier (2.0) and max mass difference (15 ppm), as previously reported (Bahja et al., 2022). HPLC alignment files were generated using MZmine (Katajamaa et al., 2006). Briefly, raw format (.raw) files were imported and features were detected with the mass detection algorithm (MS level 1, noise level 1×10^5). Chromatogram construction was performed using the ADAP chromatogram builder (Myers et al., 2017; Pluskal et al., 2010): minimum group scan size (3), minimum group intensity (1×10^3), minimum highest intensity (1×10^5), and mass/charge (*m/z*) tolerance (0.005 *m/z* or 10 ppm). Chromatogram deconvolution was carried out using a local minimum search algorithm: chromatographic threshold (0.02%), search minimum in retention time (RT) threshold (0.05 min), minimum relative peak height (0.02%), minimum absolute height (5×10^5), minimum ratio of peak/top edge (3), and peak duration range (0.05 to 1.5 min). Isotopic peak grouping utilised (*m/z* tolerance 0.005 *m/z* or 10 ppm, RT tolerance 0.05 min, maximum

charge 2) the most intense isotope used as a representative. Join alignment was performed (m/z tolerance 10ppm, m/z weight 20, RT tolerance 0.1 min, weight for RT 20) with gap filling (same RT and m/z range gap filler), m/z tolerance (10ppm). After filtering (using the 'feature list rows filter' and setting the 'minimum peaks in a row' to 0.75 and the 'minimum peaks in an isotope pattern' as 2), data were exported as .csv file. Full details of the bioinformatic transformations required for compatibility with LipiDex software are detailed in the example data provided (Hutchins et al., 2018). Full lipidomic methodology has been published previously (Bahja et al., 2022).

Lipid quantifications were performed relative to the peak area of the isotopic standard added at the Bligh–Dyer extraction stage. PE, PE(OH), plasmanyl-PE, and plasmenyl-PE species were quantified to the PE standard 15:0–18:1(d7) PE (5.3 $\mu\text{g/mL}$), and PC, PC(OH), plasmanyl-PC, and plasmenyl-PC were quantified to the PC standard 15:0–18:1(d7) PC (150.6 $\mu\text{g/mL}$). DG, TAG, PI, PG, PS, and SM lipids were quantified relative to peak areas corresponding to 15:0–18:1(d7) DG (8.8 $\mu\text{g/mL}$), 15:0–18:1(d7)–15:0 TAG (52.8 $\mu\text{g/mL}$), 15:0–18:1(d7) PI (8.5 $\mu\text{g/mL}$), 15:0–18:1(d7) PG (26.7 $\mu\text{g/mL}$), 15:0–18:1 (d7) PS (3.9 $\mu\text{g/mL}$), and d18:1–18:1(d9) SM (29.6 $\mu\text{g/mL}$), respectively. LysoPE and LysoPC were quantified relative to peak areas corresponding to 18:1(d7) LysoPE (4.9 $\mu\text{g/mL}$) and 18:1(d7) LysoPC 23.8 $\mu\text{g/mL}$. Total lipid concentration was normalised by molar concentration across all lipid species for each sample, and final data are presented as % molar composition or lipid concentration (nanomoles/hippocampus).

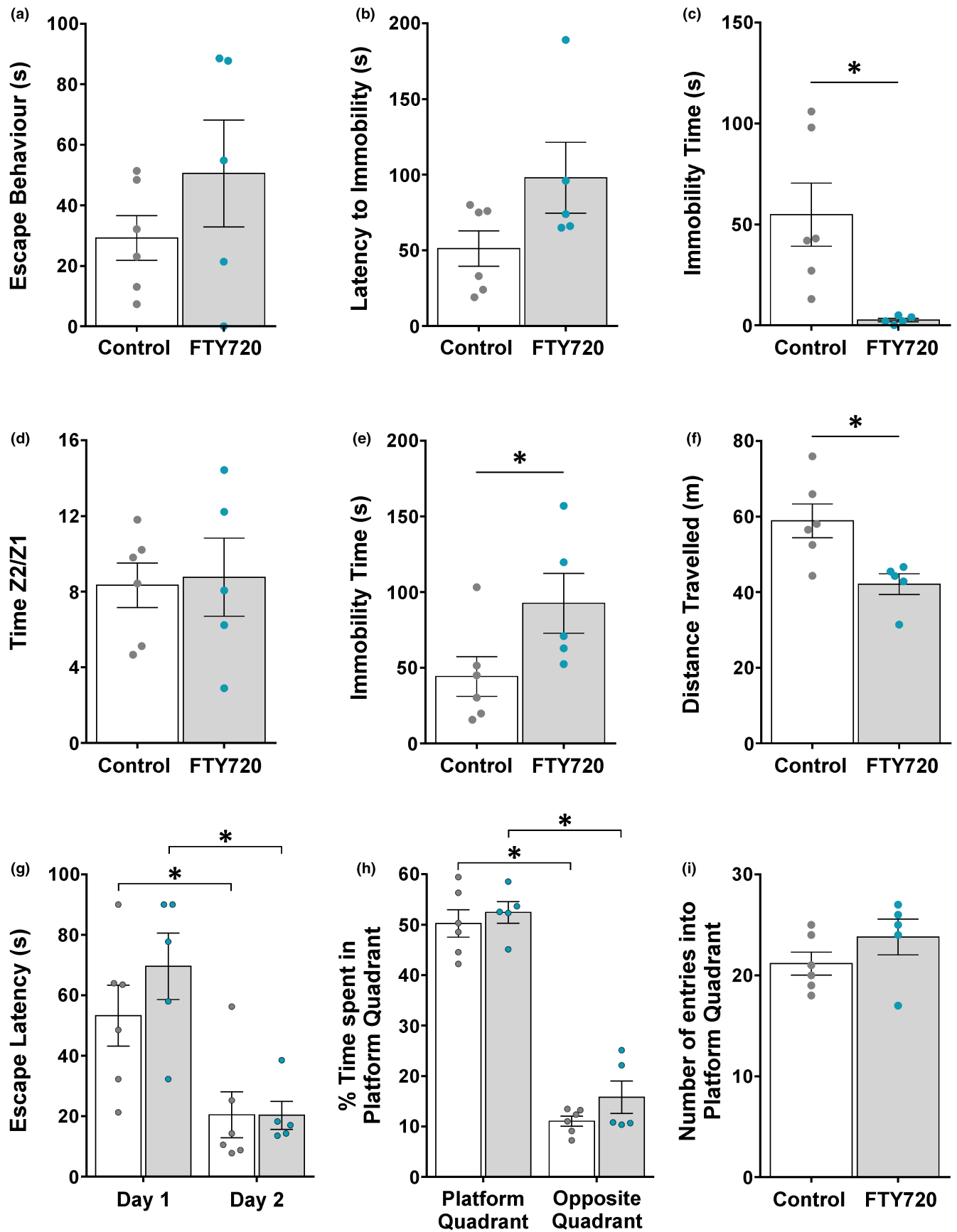
2.9 | Statistical analysis

No blinding was performed in this study. For behavioural studies, a sample size of $n=6$ per group was estimated based on our previous work (Sheridan & Dev, 2014), which reported behavioural effects of FTY720 using group sizes of five mice. One mouse in the FTY720 group was excluded from the analysis because it displayed abnormal

behaviour in the open field test and in the forced swim apparatus; that is, it hardly stopped moving in the OFT, and it hardly swam at all in the FST. For lipidomic studies, a sample size of $n=10$ was estimated based on previous published work (Fitzner et al., 2020) that used group sizes of $n=3-5$ to investigate lipidomic changes in the mouse brain. We doubled the sample size estimation in our study because of its exploratory nature and to be more confident of detecting a drug effect, if present. For lipidomic analysis, one mouse from the control group was excluded because a problem was encountered with that lipid sample during the mass spectrometry protocol and the final hippocampal lipid concentrations for that mouse were inaccurate.

The data are expressed as mean \pm SEM. All behaviour data were analysed using GraphPad Prism 10 (GraphPad Software, San Diego, CA, USA). Unpaired two-tailed Student's *t*-tests were performed for the forced swim and open field tests. Morris water maze data were analysed using two-way analysis of variance (ANOVA) and unpaired Student's *t*-test, as appropriate. The post hoc test used was Šidák's test, and a p -value <0.05 was considered statistically significant. The heatmap was generated using GraphPad Prism 10 software. For the volcano plot analysis, Perseus version 2.0.3.0 (Computational Systems Biochemistry; Tyanova et al., 2016) was used to perform Student's *t*-tests between the control and FTY720 treatment groups. A threshold value of $p < 0.05$ was considered statistically significant. In addition, lipids had to demonstrate a fold change of ≤ 0.77 or ≥ 1.3 to be considered statistically significant. Both volcano plots were generated in GraphPad Prism 10 software. A linear mixed effects model was performed on the full data set using R and the lme4 package (Bates et al., 2015) confirming a significant drug effect of FTY720. The lipidr package in R (Mohamed et al., 2020) was used to perform OPLS-DA (orthogonal partial least squares discriminant analysis) to visualise the significant FTY720-mediated drug effect. To analyse the degree of unsaturation and changes in fatty acid chain length of individual lipid classes, two-way ANOVAs were performed in GraphPad Prism 10 software with Šidák's multiple comparison correction tests. To study

FIGURE 3 FTY720 decreases immobility time in the forced swim paradigm but increases immobility and reduces total distance travelled in the open field arena. Mice were first exposed to the forced swim test on postnatal day 38 after 17 days of FTY720 treatment. (a) The amount of time that mice spent trying to climb and escape from the forced swim apparatus was calculated, and there was no statistical difference between control and FTY720-treated mice (29.2 ± 7.4 vs. 50.5 ± 17.7 s, $t=0.048$, $df=9$, $p=0.96$). (b) The time it took for mice to stop swimming initially (latency to immobility) in the forced swim apparatus was calculated, and there was no statistical difference between control and FTY720-treated mice (51.2 ± 11.7 vs. 98.0 ± 23.4 s, $t=2.098$, $df=9$, $p=0.06$). (c) The total amount of time mice spent immobile in the forced swim apparatus was calculated, and there was a statistical difference between control and FTY720-treated mice (54.8 ± 15.6 vs. 2.6 ± 0.9 s, $t=6.557$, $df=9$, $p=0.0001$). On postnatal day 39, mice were tested in the open field arena. (d) The duration of time mice spent in the central zone (Z1) and the peripheral zone (Z2) was calculated, and the ratios of time spent in zone 2 vs. zone 1 (Z2/Z1) were calculated. There was no statistical difference between control and FTY720-treated mice (8.3 ± 1.2 vs. 8.8 ± 2.1 , $t=0.106$, $df=9$, $p=0.92$). (e) The amount of time that mice spent immobile in the open field arena was calculated, and there was a statistical difference between control and FTY720-treated mice (44.2 ± 13.1 vs. 92.6 ± 19.8 s, $t=2.355$, $df=9$, $p=0.04$). (f) The total distance that each mouse travelled in the open field arena was calculated, and there was a statistical difference between control and FTY720-treated mice (58.9 ± 4.5 vs. 42.1 ± 2.8 s, $t=3.109$, $df=9$, $p=0.01$). On postnatal days 40 and 41, mice were trained in the Morris water maze spatial learning task. FTY720 did not exert any significant effects on spatial learning or memory retention in the Morris water maze paradigm. (g) The time it took for mice to find the hidden platform on day 2 decreased significantly from times recorded on day 1 (two-way ANOVA, $F(1, 18)=24.19$, $p=0.001$). (h) On postnatal day 42, the spatial memory of each mouse was tested in a probe trial. The amount of time control and FTY720-treated mice spent swimming in the platform quadrant was significantly greater than the time spent in the opposite quadrant (two-way ANOVA, $F(1, 9)=166.9$, $p=0.001$). (i) Finally, the number of times each mouse entered the platform quadrant was calculated. There was no statistical difference between control and FTY720-treated mice (21.2 ± 1.1 vs. 23.8 ± 1.8 , $t=1.17$, $df=9$, $p=0.27$). In all bar charts, vehicle control mice are depicted by white bars and FTY720-treated mice are represented by grey bars.



changes in the %mol composition of individual lipid classes, individual Student's *t*-tests were performed in GraphPad Prism 10 software. To investigate whether FTY720 exerted a dose-dependent effect on the concentration of individual lipid species, Pearson's *r* correlations were performed using GraphPad Prism 10 software (Figure 2d).

3 | RESULTS

3.1 | FTY720 decreases depression-like behaviour in the forced swim test but increases anxiety-like behaviour in the open field test

Seventeen days of treatment with FTY720 from weaning age (P21) to postnatal day 38 had a significant effect on mouse behaviour in the forced swim paradigm (Figure 3a–c). FTY720 dramatically reduced the amount of time mice spent immobile (54.8 ± 15.6 vs. 2.6 ± 0.9 s, $p=0.0001$). However, FTY720 did not significantly increase climbing or escape-like behaviour in the forced swim test (control: 29.2 ± 7.4 vs. FTY720: 50.5 ± 17.7 s, $p=0.96$). The following day (postnatal day 39), mouse behaviour was then assessed in the open field test (Figure 3d–f). Control mice spent the same proportion of time as FTY720-treated mice in the centre (zone 1) versus the borders of the arena (zone 2; 8.3 ± 1.2 vs. 8.5 ± 1.7 , respectively, $p=0.92$). Interestingly, in contrast to the forced swim test, the FTY720-treated group of mice spent over double the amount of time immobile in the open field arena compared to control mice (44.2 ± 13.1 vs. 92.6 ± 19.8 s, respectively, $p=0.04$). FTY720 also significantly reduced the total distance travelled by mice when compared to vehicle controls (58.9 ± 4.7 vs. 42.1 ± 2.8 metres, respectively, $p=0.01$). On postnatal day 40, after 19 consecutive days of FTY720 exposure, mice were trained in the Morris water maze spatial learning paradigm (Figure 3g). Both control and FTY720-treated mice demonstrated significant decreases in escape latency on training day 2 (P41), suggesting that both groups learned the spatial memory task (control: 53.3 ± 21.7 vs. 20.5 ± 8.4 s; and FTY720: 69.6 ± 28.4 vs. 20.3 ± 8.3 s). Moreover, mice treated with FTY720 spent approximately the same amount of time (ca. 50%) as control mice swimming in the platform quadrant on day 3 of the MWM test (i.e. the probe trial), suggesting that they did indeed remember the hidden platform location (Figure 3h). There were also no significant differences between control and FTY720-treated mice in the number of entries to the platform quadrant in the probe trial (Figure 3i), nor in the distance swum in 60s (data not shown). Therefore, FTY720 did not appear to exert any beneficial or detrimental effect on spatial memory.

3.2 | FTY720 exerts a significant drug effect on the mouse hippocampal lipidome

Label-free shotgun lipidomics was performed on hippocampal tissue from 6-week-old male C57BL/6 mice that were chronically treated for 3 weeks either with vehicle control or with FTY720. These mice were not exposed to any behavioural tasks. To confirm that dosing

mice with FTY720 in the drinking water resulted in a measurable accumulation of drug in the brain, mass spectrometric detection of FTY720 in hippocampal lipid samples was performed (Figure 4a–c). All ten mice demonstrated significant expression of FTY720 in the hippocampus compared to the nine controls treated with DMSO and compared to background readings (Figure 4d). In addition, a total of 599 lipid species were identified in all mice and they can be grouped into 4 main lipid categories, namely glycerolipids, glycerophospholipids, sphingolipids (i.e. sphingomyelins), and sterol lipids (i.e. cholesteryl esters; Figure 5a). The most abundant lipid classes identified (19 in total) were the phosphatidylethanolamines (PEs), the phosphatidylinositols (PIs), the plasmalogen-PE plasmalogens, and the phosphatidylcholines (PCs), whereas the least abundant lipid classes were the hydroxy-phosphatidylethanolamines (PEOHs), the alkanyl-triacylglycerols, and the alkenyl-triacylglycerols (Table 1). The heatmap in Figure 5b displays the relative abundance of each lipid class per mouse hippocampus, in both control ($n=9$) and FTY720-treated ($n=10$) groups. A linear mixed effects model suggested a significant effect of the drug, and OPLS-DA (orthogonal partial least squares discriminant analysis) confirmed that FTY720 drug-treated mice displayed a hippocampal lipid signature that diverged from control animals (Q2 value of 0.594 and R2Y value of 0.784; Figure 5c). Q2 and R2Y values represent the predictability and goodness of fit of the model, respectively.

3.3 | FTY720 reduces hydroxy-phosphatidylcholine (PCOH) monounsaturated fatty acids and increases PCOH polyunsaturated fatty acids

Saturated fatty acids (FAs) have no double bonds, while unsaturated FAs exhibit one or more double bonds (Lei et al., 2016) and can be further classified into monounsaturated fatty acids (MUFAs) and polyunsaturated fatty acids (PUFAs). We analysed the effects of FTY720 on the degree of unsaturation of all identified lipid classes in the mouse hippocampus (Figure 6). When analysing the total lipid content, we found that FTY720 caused a significant increase in the proportion of lipids possessing 3–4 carbon–carbon double bonds (Figure 6a). We then investigated the saturation status of each lipid class individually. Hydroxy-phosphatidylcholine (PCOH) MUFAs containing one double bond were reduced following 3 weeks of FTY720 drug treatment (control: $9.4 \pm 1.3\%$ vs. FTY720: $5.9 \pm 0.2\%$, $p=0.018$; Figure 6c), whereas there was a concomitant increase in PCOH-PUFAs containing two or more double bonds (control: $87.9 \pm 1.7\%$ vs. FTY720: $92.4 \pm 0.3\%$, $p=0.002$). There were no significant changes in the degree of unsaturation of any other lipid classes identified.

3.4 | FTY720 increases the fatty acid chain length of hydroxy-phosphatidylcholine lipids

Fatty acids can also be classified by their hydrocarbon chain length and the number of carbon–carbon bonds present. For example,

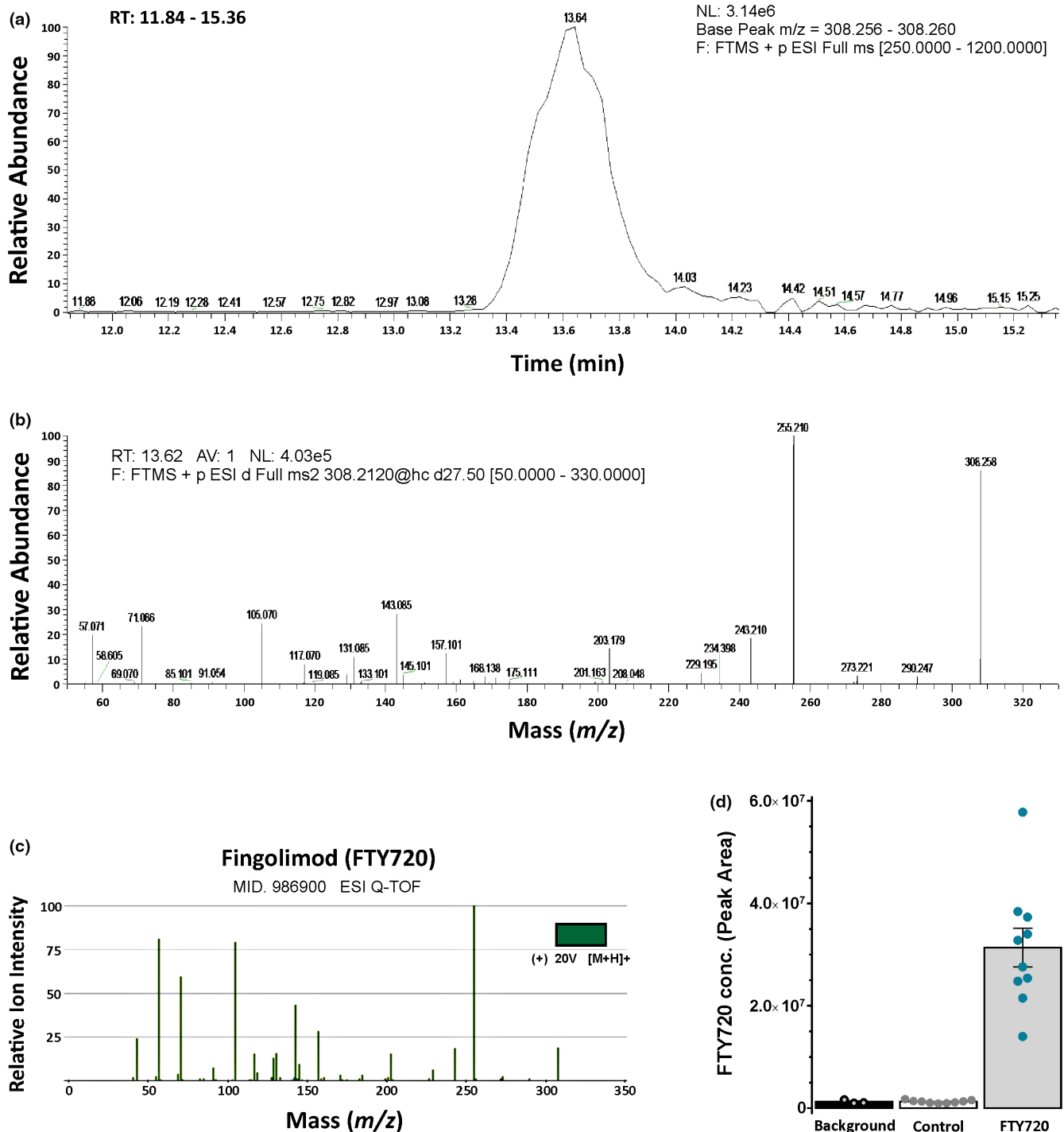


FIGURE 4 Detection of FTY720 in the mouse hippocampus using liquid chromatography–mass spectrometry. (a) Mass spectrum of a hippocampal tissue sample from a mouse treated with FTY720 for 3 weeks. The base peak mass-to-charge ratio (m/z) of 308.256–308.260 was detected at a retention time (RT) of 13.62 min. (b) Collision-assisted dissociation mass spectra of FTY720 (m/z 308.3 → 255.2; Xue et al., 2020). (c) Relative ion intensity peak of 308.3 confirms the presence of FTY720 (fingolimod) in the drug-treated brain tissue samples. (d) The relative concentration of FTY720 for each drug-treated mouse was calculated as the peak area and compared to background levels and to control hippocampal tissue samples. There were no differences between DMSO vehicle control-treated mice and background, whereas FTY720-treated mice, on average, displayed ca. 25 times larger peak areas, confirming the presence of FTY720 in hippocampal tissue samples.

short-chain FAs possess 2–5 carbon atoms; medium-chain FAs, 6–12 carbons; long-chain FAs, 13–21 carbons; and very long-chain FAs, ≥22 carbons (Lei et al., 2016). We analysed the effects of FTY720 exposure

on the FA hydrocarbon chain length of all lipids identified in the mouse hippocampus (Figure 7). A small proportion (2.6–2.7%) of the lipids identified could be classed as long-chain FAs possessing 14–20

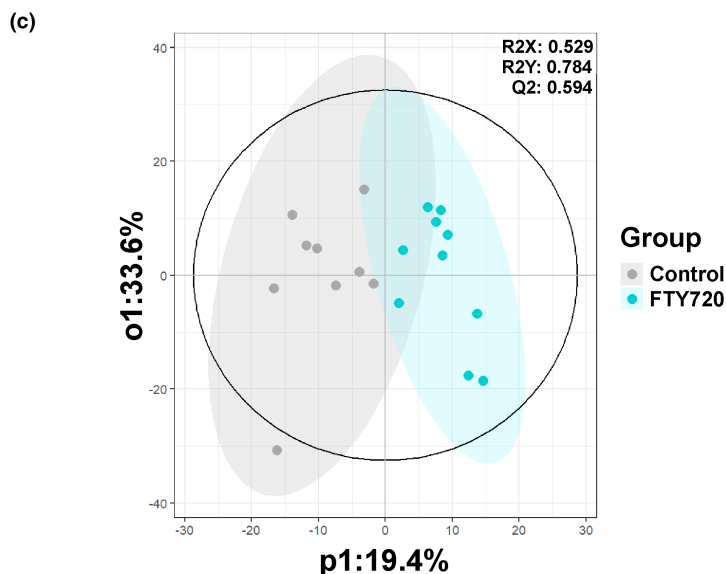
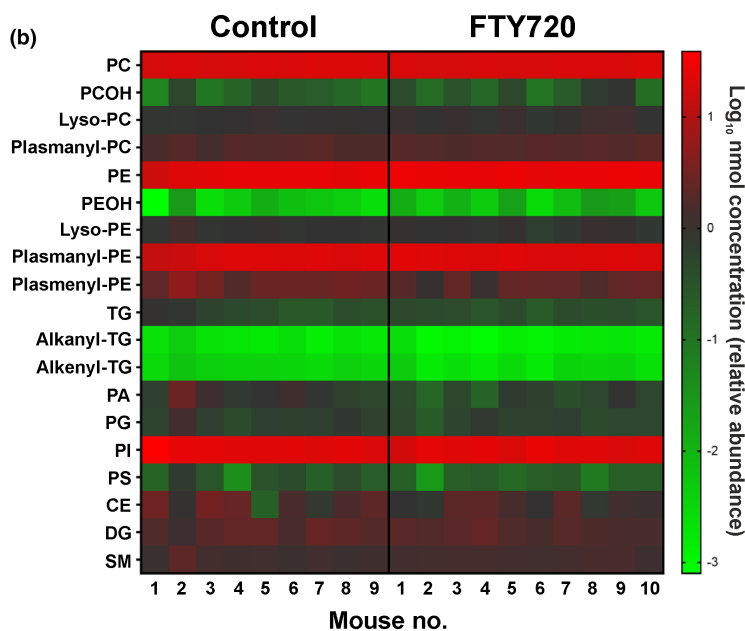
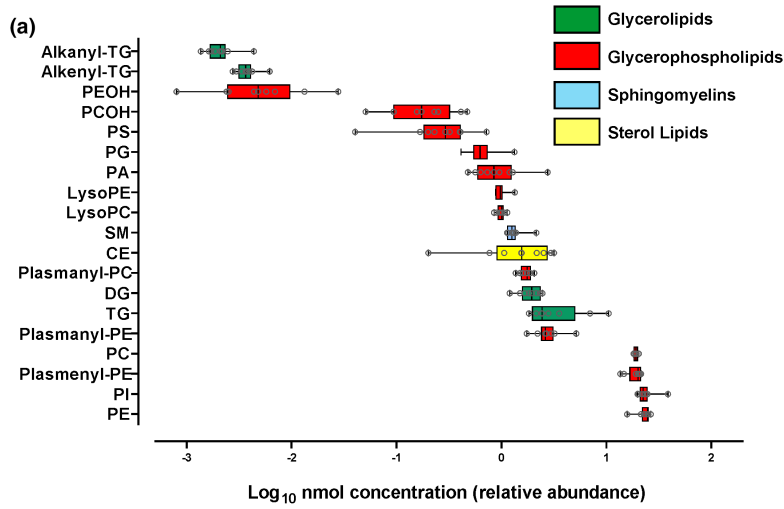


FIGURE 5 Chronic FTY720 treatment alters hippocampal lipid expression. (a) Horizontal boxplots displaying the dynamic range of lipid class expression in the mouse hippocampus. The relative abundance of four lipid categories (glycerolipids, glycerophospholipids, sphingolipids (i.e. sphingomyelins), and sterol lipids) comprised of 19 lipid classes, and a total of 599 lipid species are expressed as Log_{10} nanomolar concentrations. (b) A heatmap showing the relative expression of each lipid class for every mouse hippocampus in the control ($n=9$) and FTY720-treated ($n=10$) groups. (c) OPLS-DA (orthogonal partial least squares discriminant analysis) plot illustrating a significant effect of FTY720 drug treatment. The goodness of fit and predictability of the model are represented by $R^2X=0.529$, $R^2Y=0.784$, and $Q^2=0.594$. CE, cholesteryl ester; DG, diacylglycerol; LysoPC, lysophosphatidylcholine; LysoPE, lysophosphatidylethanolamine; PA, phosphatidic acid; PC, phosphatidylcholine; PCOH, hydroxy-phosphatidylcholine; PE, phosphatidylethanolamine; PEOH, hydroxy-phosphatidylethanolamine; PG, phosphatidylglycerol; PI, phosphatidylinositol; PS, phosphatidylserine; SM, sphingomyelin; TG, triacylglycerol.



carbons (Figure 7a), whereas the vast majority were very long-chain FAs possessing ≥ 22 carbons. There were no changes in the overall proportions of FA chain lengths following FTY720 treatment (Figure 7a). Interestingly, we found an increase in the expression of hydroxy-phosphatidylcholine lipid species containing 38-carbon FA chains (control: $30.0 \pm 2.2\%$ vs. FTY720: $35.7 \pm 0.9\%$, $p=0.0003$; Figure 7c). Since the data are expressed as a proportion, if one FA chain length significantly increases following FTY720 exposure, then the other hydrocarbon chain lengths should decrease as a result. Following that logic, it appeared as though there was a concomitant decrease in the expression of PCOH lipid species containing 34 carbons (control: $9.0 \pm 1.2\%$ vs. FTY720: $5.8 \pm 0.2\%$, $p=0.11$). However, the multiple comparison-adjusted p -value was not statistically significant. There

were no significant changes in the FA hydrocarbon chain length of any of the other lipid classes identified.

3.5 | Chronic oral treatment with FTY720 significantly increases expression of 99 distinct lipid species in the mouse hippocampus

A total of 599 distinct lipid species were detected by LC-MS in mouse hippocampal tissue samples (Table 1): 423 belonged to the category of glycerophospholipids, 37 were sphingomyelins, 134 were glycerolipids, and 5 were cholesteryl esters. We analysed the effect of chronic FTY720 exposure on the expression of each of the 599

TABLE 1 Lipid categories and lipid classes identified in the mouse hippocampus by label-free shotgun lipidomic methods.

Lipid categories and lipid classes	Number of lipid species	Sum total (nmol/hippocampus)
Glycerophospholipids		
Phosphatidylcholine (PC)	117	62.82 ± 12.34
Hydroxy-phosphatidylcholine (PCOH)	66	0.64 ± 0.34
Lysophosphatidylcholine (LysoPC)	20	3.26 ± 0.73
Phosphatidylethanolamine (PE)	55	76.54 ± 19.11
Hydroxy-phosphatidylethanolamine (PEOH)	9	0.02 ± 0.01
Lysophosphatidylethanolamine (LysoPE)	15	3.16 ± 0.48
Phosphatidylinositol (PI)	18	80.18 ± 30.88
Phosphatidic acid (PA)	4	3.09 ± 1.11
Phosphatidylglycerol (PG)	15	2.10 ± 0.29
Phosphatidylserine (PS)	3	0.91 ± 0.40
Plasmany-PC	40	5.62 ± 1.25
Plasmany-PE	12	8.91 ± 1.22
Plasmenyl-PE	49	62.91 ± 16.90
Total	423	310.16
Sphingolipids		
Sphingomyelin (SM)	37	4.24 ± 0.52
Total	37	4.24
Glycerolipids		
Triacylglycerol (TG)	90	1.62 ± 0.99
Alkanyl-TG	7	0.0068 ± 0.0015
Alkenyl-TG	4	0.012 ± 0.021
Diacylglycerol (DG)	33	6.48 ± 2.06
Total	134	8.12
Sterol lipid		
Cholesteryl ester (CE)	5	6.21 ± 4.23
Total	5	6.21
Total	599	328.73

Note: A total of 599 lipid species were identified, including 423 distinct glycerophospholipids that made up 94% of the total lipid concentration of the hippocampus. The most abundant lipid classes were the phosphatidylinositols (PI, 24% total lipid composition), phosphatidylethanolamines (PE, 23%), plasmenyl-PE (19%), and phosphatidylcholines (PC, 19%). A total of 37 very long-chain fatty acid sphingomyelin (SM) lipid species were identified, as well as 5 long-chain fatty acid cholesteryl ester (CE) lipids.

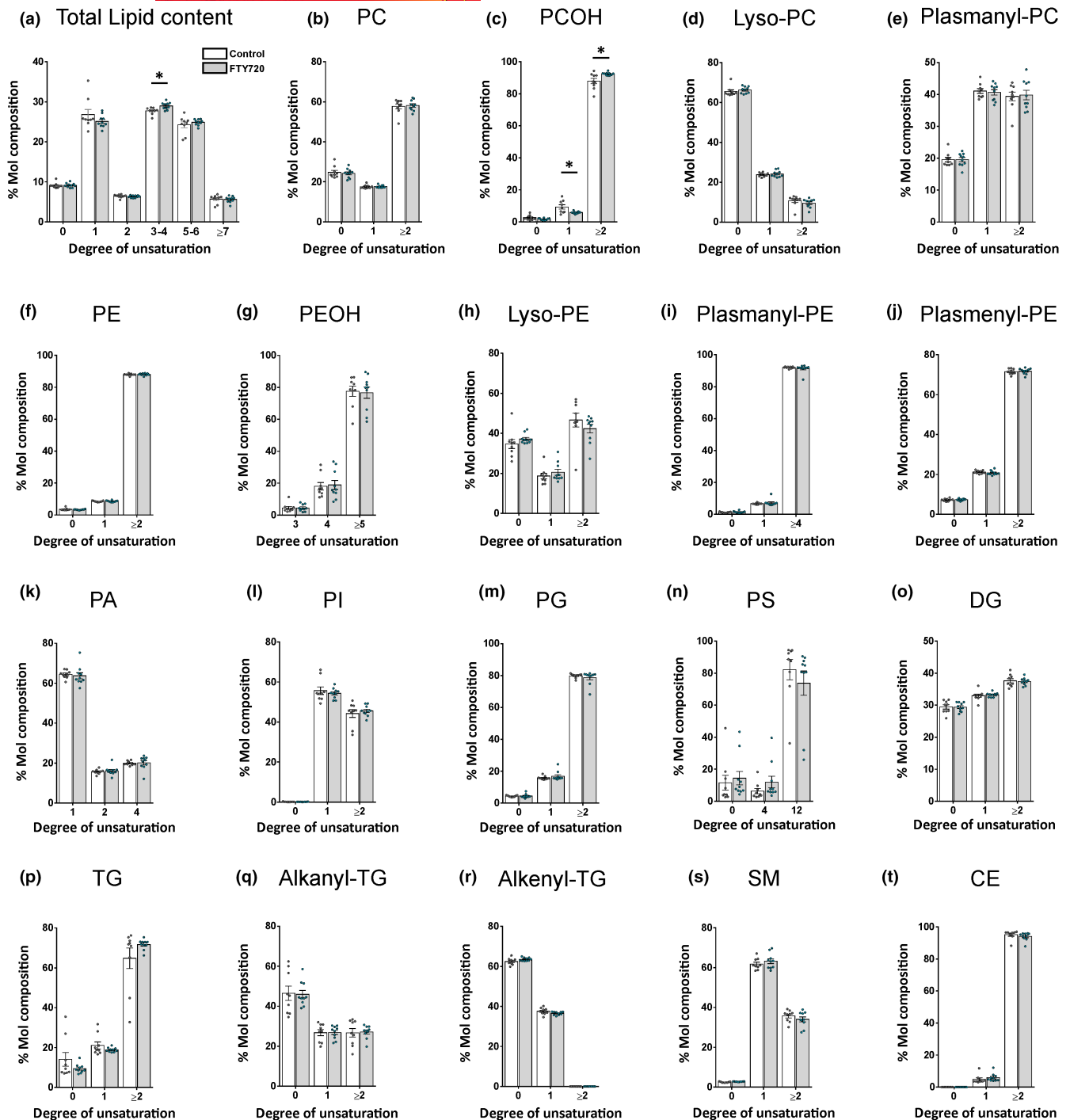


FIGURE 6 FTY720 treatment leads to a decrease in monounsaturated FAs and an increase in polyunsaturated FAs of the PCOH lipid class in the mouse hippocampus. (a) Changes to the saturation status of all lipid species identified in the hippocampus of control and FTY720-treated mice were analysed. Polyunsaturated fatty acids containing 3 or 4 carbon double bonds were significantly elevated in drug-treated mice (unpaired Student's *t*-tests with Holm-Šidák's corrections for multiple comparisons, $t=3.099$, $p=0.007$). (b)–(t) The degree of unsaturation of each of the 19 distinct lipid classes was also analysed in both control and FTY720-treated mice. Each of the 599 lipid species was described as 'saturated' (fatty acid hydrocarbon chains containing zero double bonds), 'monounsaturated' (FA chains containing one double bond), or 'polyunsaturated' (FA chains containing two or more double bonds). The degree of unsaturation was expressed as a percentage (%) of the total molecular composition of that particular lipid class. White bars represent control animals, and grey bars represent FTY720-treated mice. (c) 3 weeks of exposure to FTY720 caused a decrease in MUFAs (Šidák's multiple comparison post hoc test, $p=0.018$) and an increase in PUFAs (Šidák's multiple comparison post hoc test, $p=0.002$) of the hydroxy-phosphatidylcholine (PCOH) lipid class (two-way ANOVA, $F(2, 51)=6511$, $p=0.0001$). FTY720 did not alter the degree of saturation of any other lipid class.

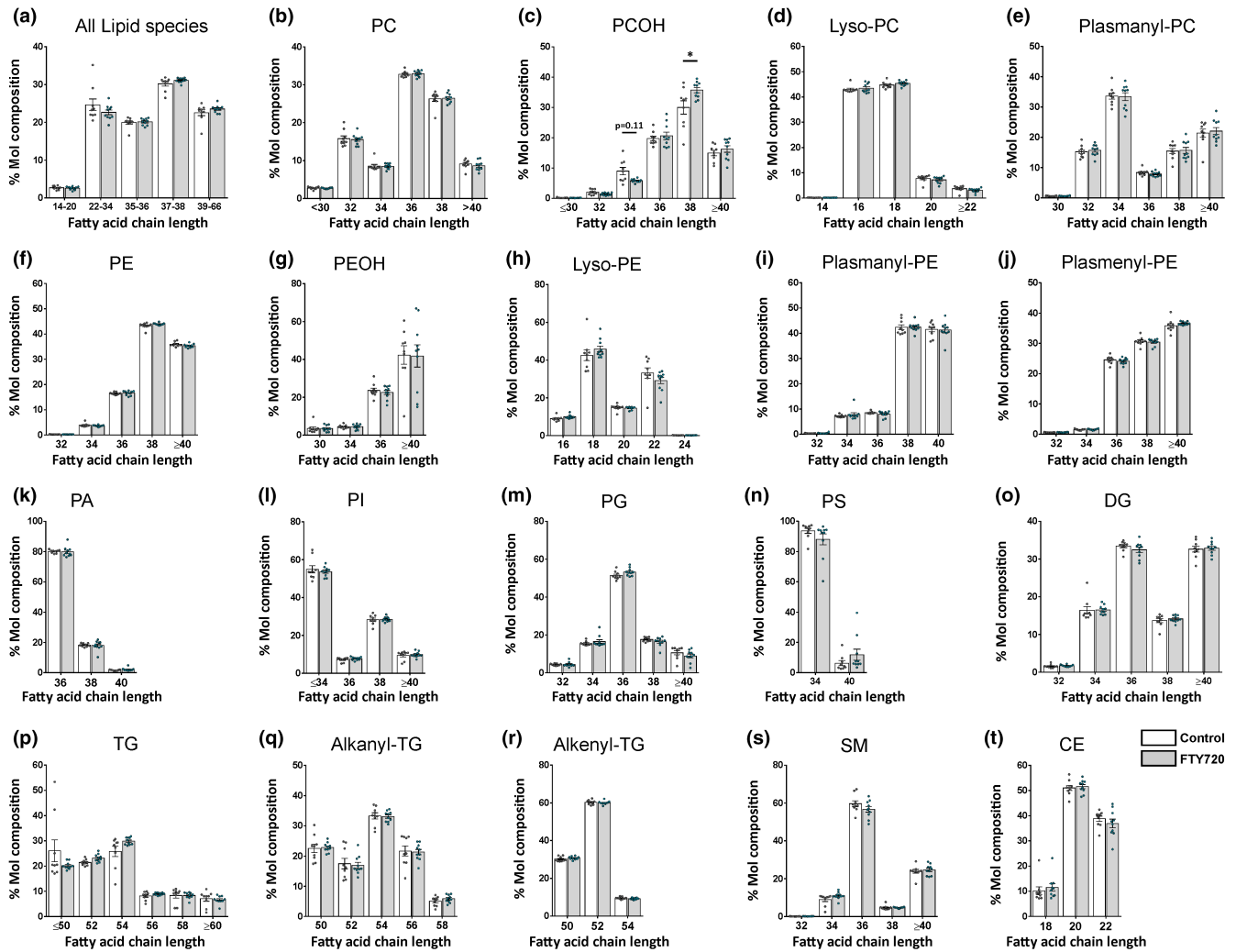


FIGURE 7 FTY720 treatment caused an increase in the fatty acid chain length of hydroxy-phosphatidylcholine (PCOH) lipids in the mouse hippocampus. (a) 599 lipid species were identified by HPLC-MS, belonging to 19 separate lipid classes. Long-chain FAs (14–21 carbons) comprised approximately 2.6–2.7% of total lipids, and the remaining were very long-chain FAs with 22- to 66-carbon chain lengths. FTY720 did not cause an overall change in FA hydrocarbon chain length in the mouse hippocampus. (b)–(t) Each lipid class was composed of lipids that displayed a range of FA hydrocarbon chain lengths. Most of the lipid classes were composed of lipid species with very long-chain FAs (i.e. ≥ 22 hydrocarbons), apart from (c) LysoPC, (g) LysoPE, and (s) CE, which predominantly contained long-chain FAs (14–20 carbon atoms). (c) FTY720 caused an increase in the proportion of PCOH lipids with a FA hydrocarbon chain length of 38 (two-way ANOVA, $F(5, 102) = 344$, Šidák's multiple comparison post hoc test, $p = 0.0003$). It appeared that FTY720 may also cause a decrease in the proportion of PCOH lipids with a FA chain length of 34 carbons; however, the multiple comparison-adjusted p -value was not significant (Šidák's post hoc test, $t = 2.376$, $p = 0.11$). FTY720 did not alter the FA chain length of any other lipid class.

lipid species identified by plotting the $-\log_{10}(p\text{-value})$ against the $\log_2(\text{fold change})$, as represented by the volcano plot (Figure 8a). 161 lipid species were significantly altered following 3 weeks of exposure to FTY720. However, we then set more stringent criteria that also considered the magnitude of the fold change. Only lipid species that demonstrated a fold change of ≥ 1.3 or ≤ 0.77 were considered significant. Based on these criteria, 99 lipid species were up-regulated and 3 lipid species were down-regulated following FTY720 exposure (Figure 8b). When the individual lipid species were grouped into their respective lipid classes, there was a significant up-regulation in plasmeynyl-PE plasmalogens (Figure 8f). The plasmeynyl-PE lipid class composes $17.0 \pm 1.3\%$ of the total molar composition of lipids in the

hippocampus of control mice, and this increased to $20.5 \pm 0.9\%$ Mol composition (t -test, $p = 0.035$, Figure 8f) following FTY720 exposure. On the contrary, there was a significant decrease in phosphatidic acid (PA) lipids 3 weeks post-FTY720 treatment. The PA lipid class composes $1.1 \pm 0.2\%$ of the total molar composition of lipids in the hippocampus of control mice, and this decreased to $0.5 \pm 0.07\%$ Mol composition (t -test, $p = 0.019$, Figure 8i) following FTY720 exposure. Table S1 provides a comprehensive list of the individual lipid species that were significantly up- or down-regulated in expression in the mouse hippocampus following 3 weeks of oral FTY720 exposure. Among them are 18 sphingomyelin lipid species that display fold changes between 1.32 and 1.76 in FTY720-treated mice.

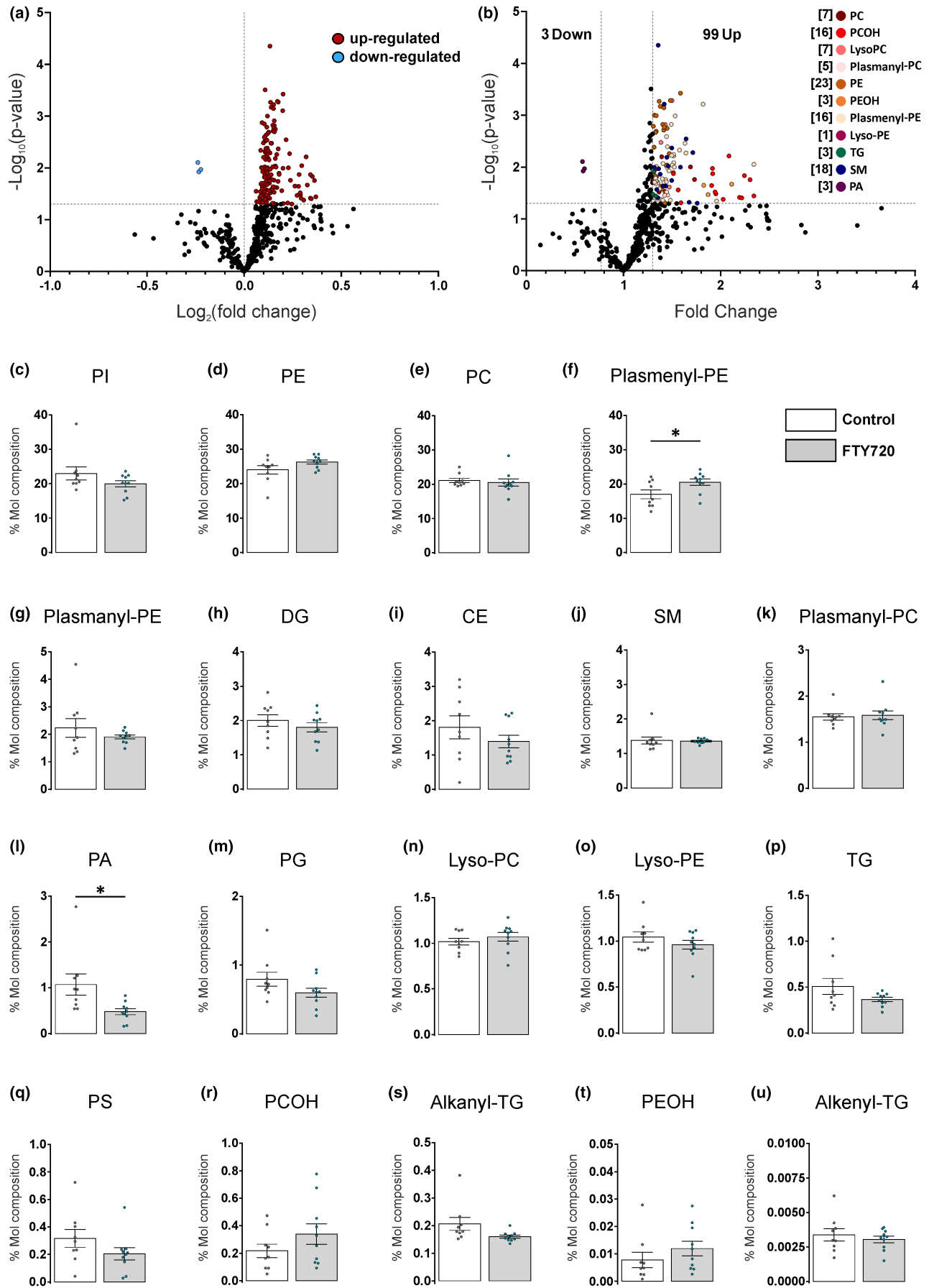


FIGURE 8 FTY720 effects on the expression of lipids in the mouse hippocampus. (a) Volcano plot of individual lipid species. The negative Log_{10} of the p -value (Y-axis) is plotted against the Log_2 of the fold change in lipid expression of FTY720-treated mice versus the control group. Black dots represent no significant change ($p > 0.05$) with FTY720 treatment, the blue dots represent down-regulated lipids, and red dots represent up-regulated lipids. (b) When a fold change cut-off of ≥ 1.3 or ≤ 0.77 is also applied to the data in addition to the p -value threshold, the number of lipid species that met these criteria decreased and is represented by the coloured dots. Individual lipid species are listed in [Table S1](#). (c)–(u) Lipid composition of hippocampus of control mice (white bars) or mice treated with FTY720 (grey bars). Graphed on the Y-axes are the percentage (%) molar compositions. Values are mean \pm SEM. Control ($n = 9$) and FTY720 ($n = 10$) mice per group. Statistical analyses were performed using unpaired two-tailed Student's t -tests, $*p < 0.05$. FTY720 caused an increase in (f) plasmeyl-PE lipids (t -test, $t = 2.283$, $df = 17$, $p = 0.035$) and a concomitant decrease in (l) phosphatidic acid lipids (t -test, $t = 2.591$, $df = 17$, $p = 0.019$).

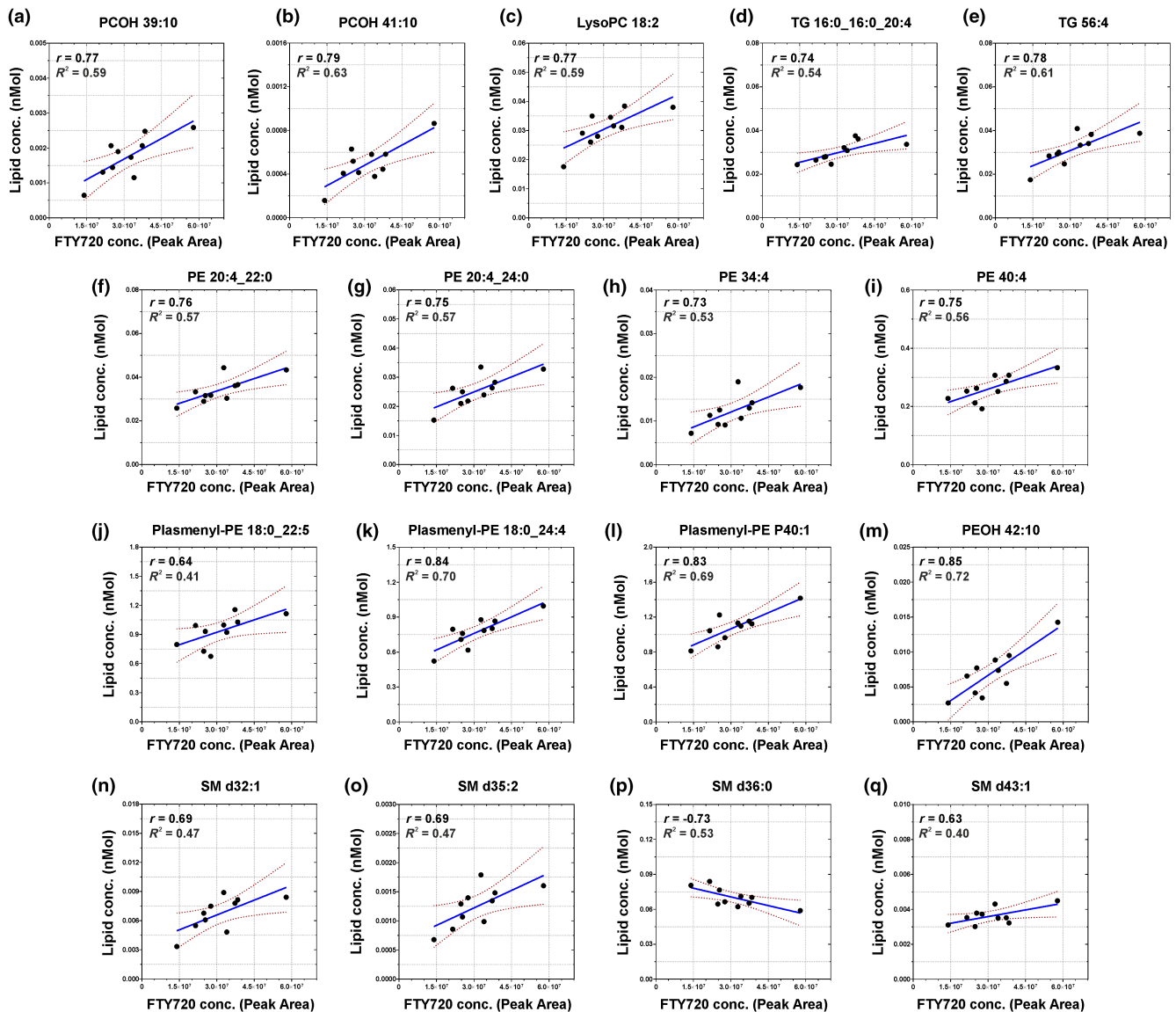


FIGURE 9 Hippocampal FTY720 concentration versus lipid concentration. A total of 102 lipid species demonstrated significant changes in expression following 3 weeks of FTY720 exposure. 17 of those lipids demonstrated a dose-dependent regulation of their expression levels. (a, b) Two hydroxy-phosphatidylcholine (PCOH) lipid species demonstrate a dose-dependent increase in concentration, as does (c) LysoPC 18:2. Similarly, both (d) TG 16:0_16:0_20:4 and (e) TG 56:4 display positive correlations with hippocampal FTY720 concentration (calculated as peak area). (f–i) Four phosphatidylethanolamine (PE) lipids display dose-dependent increases in concentration, and (j–l) three plasmeyl-PE plasmalogens also show positive correlations with hippocampal FTY720 levels. (m) PEOH 42:10 demonstrates the strongest positive relationship with hippocampal FTY720 concentration (Pearson's $r = 0.85$, $R^2 = 0.72$). (n–o) Both SM d32:1 and SM d35:2 sphingomyelins display a dose-dependent increase in expression following 3 weeks of FTY720 exposure, whereas (p) SM d36:0 sphingomyelin is the only lipid to show a dose-dependent decrease in concentration (Pearson's $r = -0.73$, $R^2 = 0.53$). Finally, (q) SM d43:1 displays a moderate increase in concentration with increasing hippocampal FTY720 concentrations (Pearson's $r = 0.63$, $R^2 = 0.40$).



3.6 | Several lipid species display dose-dependent changes in expression following FTY720 exposure

Finally, since label-free shotgun lipidomics enabled us to detect the relative abundance of FTY720 in each mouse hippocampus, we investigated whether any of the significantly changing lipid species also demonstrated dose-dependent regulation of their expression levels. Using Pearson's *r* correlation analysis, we plotted the abundance (peak area) of FTY720 in each mouse hippocampus against the nanomolar concentration of each lipid and found that 17 out of 102 lipids displayed dose-dependent changes in expression (Figure 9). Interestingly, 16 lipid species demonstrated positive correlations and only one showed a negative correlation; that is, as FTY720 levels increased, the concentration of that single lipid decreased (Figure 9p). The three most abundant lipid species that displayed positive correlations and dose-dependent increases in expression were the plasmalogens, Plasmalogen-PE 18:0_22:5 (Pearson's $r=0.64$; Figure 9j), Plasmalogen-PE 18:0_24:4 (Pearson's $r=0.84$; Figure 9k), and Plasmalogen-PE P40:1 (Pearson's $r=0.83$; Figure 9l). Three sphingomyelin lipid species also demonstrated dose-dependent increases in expression because of FTY720 accumulation in the hippocampus, namely SM d32:1 (Pearson's $r=0.69$; Figure 9n), SM d35:2 (Pearson's $r=0.69$; Figure 9o), and SM d43:1 (Pearson's $r=0.63$; Figure 9q). Sphingomyelin SM d36:0, on the contrary, displayed a dose-dependent decrease in expression with increasing FTY720 accumulation in the hippocampus (Pearson's $r=-0.73$; Figure 9p). Further research will be necessary to investigate whether these 17 lipid species, in particular, are important mediators of FTY720's myriad actions on different cell types in the central nervous system.

4 | DISCUSSION

In the present study, we have investigated the impact of chronic FTY720 drug treatment on both adolescent mouse behaviour and the lipidomic signature of the hippocampus. FTY720 was the first oral disease-modifying therapy for relapsing–remitting multiple sclerosis (Brinkmann et al., 2010; Sharma et al., 2011) and is now approved for use in children and adolescents over the age of 10. As such, studying the CNS effects of FTY720 at this key stage in brain maturation is timely and clinically relevant. Because of its high oral bioavailability (>90%), lipophilic properties, and relatively long half-life (6–9 days in humans; David et al., 2012), FTY720 can cross the blood–brain barrier and accumulate in lipid-rich areas of the brain and spinal cord, particularly in white matter tracts (Dev et al., 2008; Foster et al., 2007; Hunter et al., 2016). Using mass spectrometry, our measurements confirmed that FTY720 was present in the hippocampus of chronically treated mice at ca. 25 times above background levels (Figure 4). FTY720 has been shown to have beneficial effects on cognition in a number of animal models of CNS disorders, such as schizophrenia (Yu et al., 2023), multiple sclerosis (de Bruin et al., 2016; dos Santos et al., 2019), stroke (Nazari et al., 2016), Alzheimer's disease (Asle-Rousta et al., 2013; Fagan

et al., 2022; Fukumoto et al., 2014; Kartalou et al., 2020), Parkinson's disease (Vidal-Martinez et al., 2019), Huntington's disease (Miguez et al., 2015), and even radiation-induced cognitive deficits (Stessin et al., 2017). Here, however, we found no obvious effects of FTY720 on adolescent mouse behaviour in the Morris water maze spatial learning task. This is not so surprising given that young healthy mice were used. Therefore, we can conclude that FTY720, in our hands, does not act as a nootropic agent in the strict sense of the definition, as it failed to enhance spatial memory over and above normal levels in young wild-type male mice. FTY720 did, however, decrease the amount of time that mice spent immobile in the forced swim test (FST). In recent years, the FST has received a lot of criticism regarding the types of mouse behaviours it can measure and the conclusions that can be drawn from calculating how long mice spend immobile, or alternatively, how long they spend struggling to escape (Molendijk & de Kloet, 2019; Reardon, 2019; Yankelevitch-Yahav et al., 2015). For example, we could infer from our results that FTY720 decreases depression or despair-like behaviour in adolescent mice (Figure 3c). However, the (non-significant) increase in climbing and escape-like behaviour in two out of five FTY720-treated mice could also indicate an increase in anxiety in the novel water environment. Coupled with results from the open field test, that is, a significant decrease in locomotion (Figure 3f) and a doubling of the time spent immobile (Figure 3e), it could be argued that FTY720 induces anxiogenic behaviours in adolescent male mice. On the contrary, others have shown anti-depressant (di Nuzzo et al., 2015; Guo et al., 2020) and anxiolytic (Guo et al., 2020) effects of FTY720 in classic mouse models of depression and chronic stress. In our hands, however, FTY720 appears to exert negative effects on behaviour in young healthy (non-depressed) wild-type mice, a plausible result given its potent immunosuppressant actions (Gräler & Goetzl, 2004) and the fact that the neural centres of the brain responsible for emotion, impulse control, and mood regulation are still maturing in adolescent mice during this three-week time window post-weaning (Hammelrath et al., 2016; Semple et al., 2013). Previously, using young adult female mice (11 weeks old), we have shown that FTY720 rescues locomotion deficits in the experimental autoimmune encephalomyelitis (EAE) model of multiple sclerosis (Sheridan & Dev, 2014). So, depending on whether mice are ill or healthy, FTY720 may exert opposing effects on mouse locomotion. Therefore, from a clinical perspective, the results we present here suggest that physicians should be mindful of potential adverse effects of FTY720 on mood and behaviour when conducting clinical trials and investigating the potential beneficial effects of FTY720 for non-life-threatening conditions (e.g. chemotherapy-induced neuropathic pain; National Library of Medicine [NLM], 2019, NCT03943498). In non-depressed patients, adverse drug reactions that impact mood and increase anxiogenic behaviour can often mask any modest analgesic effects of the same drug (Leung et al., 2022).

In addition to its numerous direct S1P receptor-mediated actions on neurons (Di Menna et al., 2013; Oyama et al., 1998; Rossi et al., 2012), astrocytes (Groves et al., 2013; Miron et al., 2008; Mullershausen et al., 2007; Osinde et al., 2007; O'Sullivan et al., 2018;

Wu et al., 2013), microglia (Groves et al., 2013; Nayak et al., 2010; O'Sullivan et al., 2018; Qin et al., 2017), oligodendrocytes (Groves et al., 2013; Miron et al., 2008), and cerebrovascular endothelial cells (Brinkmann, 2007; Brinkmann et al., 2004; Zhao et al., 2018), FTY720 may also impact cell signalling pathways by interacting with phospholipid membranes. FTY720 is an amphipathic molecule, possessing both hydrophobic and hydrophilic groups that incorporate into lipid bilayers. In aqueous solutions, FTY720 forms micellar aggregates that can interact with biological membranes and modulate lipid packing, thus affecting membrane permeability, stiffness, and fluidity (Swain et al., 2013). For example, FTY720, at high concentrations, has been shown to induce externalisation of phosphatidylserine (PS) in the outer membrane leaflet of tumour cell lines, leading to cell death (Young et al., 2019). In addition to its impact on the biophysical properties of the outer cell membrane, FTY720 may regulate the composition and properties of organelle membranes, including the Golgi apparatus, endoplasmic reticulum, endosomes, and mitochondria (Breslow & Weissman, 2010; Hagihara et al., 2020; Nagahara et al., 2000). S1P receptor-independent up-regulation of reactive oxygen species (ROS) has been proposed to underlie FTY720's anti-tumorigenic actions (Takasaki et al., 2018). The concentrations of lipid metabolites in the cytosol and in subcellular compartments of neurons and glia may also be modified by FTY720-mediated inhibition of enzymes, including ceramide synthase, S1P lyase, sphingosine kinase (SphK1), and acid sphingomyelinase (Bandhuvula et al., 2005; Dawson & Qin, 2011; Lahiri et al., 2009; Lim et al., 2011). For example, FTY720 reportedly inhibits the up-regulation of ceramide in the retina in response to high-intensity light exposure, thus promoting neuroprotection (Chen et al., 2013).

4.1 | Effects of FTY720 on membrane phospholipids

The goal of this study was to investigate the effects of FTY720 on the lipid content of the hippocampus of young healthy (control) mice whose brains are at a key stage of functional maturation. The composition of the phospholipid bilayer impacts membrane biophysics (Dymond, 2021) and thus the conformational flexibility of receptor complexes, as well as the opening and closing probabilities of transmembrane ion channels involved in neurotransmission and synaptic plasticity (Aureli et al., 2015; Olsen & Færgeman, 2017). The dry weight of the brain is comprised of approximately 50% lipids (Chang et al., 2009; O'Brien & Sampson, 1965; Woods & Jackson, 2006), and it has been suggested that up to 20% of the brain's energy needs are fulfilled via fatty acid oxidation, which predominantly occurs in astrocytes (Ebert et al., 2003). Fatty acids are basic lipid monomers and can exist as free FAs or as part of a complex lipid with a head group attached. The hydrocarbon chain length and the degree of unsaturation of FAs can determine the biophysical properties of phospholipid membranes. Moreover, because fatty acids usually contain double bonds in the *cis* configuration under physiological conditions, unsaturated lipids can cause an increase in the

volume of the plasma membrane while simultaneously lowering its density (Samuli Ollila et al., 2007). Therefore, a change in the length of FA chains or their ability to pack tightly together could modify membrane curvature or rigidity and potentially influence neuronal functioning in the hippocampus, for example, via modified responsiveness of transmembrane receptors to ligand binding or altered ion channel kinetics (Carta et al., 2014). Here, we report a decrease in the monounsaturated FA component and a concomitant increase in polyunsaturated FAs of hydroxy-phosphatidylcholine (PCOH) lipids following FTY720 exposure (Figure 6c). Unsaturated fatty acids can increase membrane fluidity, and so a decrease in MUFA-PCOH with a commensurate increase in PUFA-PCOH lipids could indicate a decrease in the rigidity of neuronal or glial cell membranes in the hippocampus. Interestingly, it has been shown that increasing membrane fluidity, by enriching cell membranes with PUFAs, promotes the non-amyloidogenic cleavage of amyloid precursor protein (APP) by α -secretase enzymes, thus inhibiting $A\beta_{1-42}$ accumulation and enhancing neuroprotection (Yang et al., 2011, 2014). This could explain how FTY720 leads to a reduction in APP and phosphorylated tau and acts to dampen neuroinflammation in the hippocampus of the 3xTg-AD mouse model of Alzheimer's disease (Fagan et al., 2022).

Polyunsaturated FA chains tend to occupy a larger volume at the lipid-water interface than monounsaturated or saturated FA chains, suggesting that PUFAs are curled and able to easily switch between different conformations of equivalent energies (Antonny et al., 2015). The conformational flexibility of PUFAs facilitates fast and sudden changes in transmembrane protein shape, for example, the movement of α -helices in the rhodopsin G protein-coupled receptor expressed in rod cells of the retina (Gawrisch & Soubias, 2008). PUFAs may also adapt their flexible conformations to a bent plasma membrane curvature, more easily than MUFAs, and thus enhance the functions of ion channels that normally bend the membrane, such as the mechanically gated cation channel Piezo1, as an example (Romero et al., 2019). Proteins and ion channel subunits embedded within the plasma membrane of cells and organelles are subjected to large anisotropic push and pull forces. Lateral membrane tensions are balanced by the repulsions between polar head groups and acyl tails of complex lipids. Modifying lipid structure or composition can alter the magnitude and direction of membrane forces and, thus, the ability of transmembrane proteins and ion channels to change shape (Lee, 2004). Whether the observed up-regulation in PCOH-PUFAs, mediated by FTY720, renders membrane proteins more 'mechanosensitive' (Caires et al., 2017; Cordero-Morales & Vásquez, 2018; Vásquez et al., 2014) or more likely to respond to their endogenous ligands in a physiologically relevant manner (Jobin et al., 2023) is as yet unknown. Interestingly, we also measured an increase in PCOH lipids possessing 38-carbon chain lengths (Figure 7c). In general, cell membranes containing longer fatty acids are more rigid and less permeable. However, approximately 88% of the PCOH lipids identified in the hippocampus of FTY720-treated mice were PUFAs, and while FTY720 increased PCOH fatty acid chain length, it also increased total PUFA composition (Figure 6a), particularly those with 3 or 4 carbon-carbon double bonds. Therefore, we hypothesise that the



aggregate mechanism of action of FTY720 may be to increase cell membrane fluidity in the mouse hippocampus, since FTY720 is a known inhibitor of ceramide synthase and a decrease in ceramide production leads to enhanced membrane fluidity in cancer cells (Szlasa et al., 2020). It is known that certain surfactants can reduce the van der Waals' interactions between FA acyl chains in the hydrophobic region of membranes, thus perturbing lipid packing and increasing membrane fluidity. At high concentrations, FTY720 can also perturb lipid packing without affecting membrane integrity (Swain et al., 2013). However, others have shown that activation of acid sphingomyelinase (SMase) can cause an increase in membrane fluidity. FTY720 is a known inhibitor of acid SMase (Dawson & Qin, 2011) and, therefore, speculating that FTY720 increases membrane fluidity in the mouse hippocampus must be treated with caution. Future work into the effects of FTY720 on neuronal and glial membrane fluidity could be investigated in more detail *in vitro* using pure or mixed cell culture systems.

4.2 | FTY720 and lipid signalling in the brain

One of the most widely studied regions of the brain, because of its known involvement in learning and memory formation, is the dorsal hippocampus (Fanselow & Dong, 2010; Klur et al., 2009; Moser et al., 1995; Pothuizen et al., 2004). Interestingly, FTY720 promotes neurogenesis in the dentate gyrus of the hippocampus, which may explain its ability to enhance spatial memory in adult male mice (8–9 weeks old) that typically exhibit lower rates of neurogenesis compared to 3- to 6-week-old mice (Sun et al., 2016). Moreover, MS patients can experience cognitive deficits because of demyelination and scarring of both grey and white matter-rich brain regions and FTY720 has been shown to improve learning and memory deficits in both mice (de Bruin et al., 2016; dos Santos et al., 2019) and humans (Comi et al., 2017; Fonseca, 2015; Kappos et al., 2015; Langdon et al., 2021; Petsas et al., 2019). Learning and memory are dependent on neurotransmitter release probability and synaptic plasticity, which, in turn, are dependent on key lipid signalling proteins at synaptic membranes (Postila & Róg, 2020). Lipids that compose the cell membrane, such as sphingolipids, are important for regulating neurotransmission and the function of ion channels involved in long-term potentiation (LTP) at the synapse (Sonnino & Prinetti, 2016; Olsen & Færgeman, 2017), for example. Therefore, lipids and lipid signalling molecules can exert direct and indirect effects on learning and memory formation, as well as mood, which are regulated by similar synaptic plasticity-associated mechanisms. Using LC/MS, we measured a significant change in 102 lipid species in the mouse hippocampus in response to 3 weeks of FTY720 treatment (Table S1; 99 lipid species were up-regulated, and 3 were down-regulated). Seven distinct phosphatidylcholine lipids (PC 16:0_24:4; PC 18:0_22:5; PC 32:2; PC 33:5; PC 36:7; PC 40:10; and PC 44:12) were up-regulated by 1.3-fold to 1.7-fold in the hippocampus of FTY720-treated mice. Phosphatidylcholine lipids have been shown to increase neurogenesis and neural plasticity (Magaquian

et al., 2021) and can enhance memory formation in rodents (Zhou et al., 2016). PC is the most abundant phospholipid in cell membrane bilayers (Müller et al., 2015), and the choline required for neurotransmission is stored as phosphatidylcholine (Blusztajn et al., 1987), thus serving as a crucial reservoir for normal brain function. PC lipids can be cleaved by phospholipase A2 (PLA2) converting them into lysophosphatidylcholines (LysoPC; Figure 10; Gauster et al., 2005), which can impact membrane permeability and membrane fluidity (Müller et al., 2015). Interestingly, seven distinct LysoPC lipids were also up-regulated in the hippocampus of FTY720-treated mice (see Table S1). LysoPC lipids made up ca. 1% of the total lipid concentration of the mouse hippocampus, and FTY720 caused a 25% increase in the LysoPC concentration from 3.26 to 4.09 nmoles/hippocampus. The increase in LysoPC lipid species in FTY720-treated animals appears to be somewhat counterintuitive since high concentrations of LysoPC can induce axonal demyelination (Ghasemi-Kasman et al., 2022; Velasco-Estevéz et al., 2020; Yazdi et al., 2015), and yet FTY720 can inhibit the degeneration of CNS white matter (Sheridan & Dev, 2012). LysoPC levels are also increased following traumatic brain injury (Tzekov et al., 2016) and post-spinal cord injury (Hanada et al., 2012) and are high in the cerebrospinal fluid (CSF) of MS patients (Pieragostino et al., 2015). The fact that FTY720 is an FDA-approved therapeutic for treating relapsing–remitting MS and has been shown to inhibit phospholipase A2 (PLA2; Payne et al., 2007) suggests that, in theory, FTY720 should decrease LysoPC levels. However, the somewhat modest increases in LysoPC lipids observed in our young healthy mice may not be sufficient to induce CNS pathology and are thus, most likely, not a cause for concern.

Notably, there were 15 lipid species that demonstrated fold change increases between 1.9 and 2.3 in response to chronic FTY720 exposure (Table S1), and twelve of these top-changing lipids can be classed as hydroxy-phosphatidylcholines (PCOHs). Oxidised lipids are often found to be elevated under inflammatory physiological settings (Chang et al., 2002). Many oxidised lipids are bioactive compounds that can contribute to diseases involving oxidative stress, for example, atherosclerosis (Que et al., 2018), renal ischaemia (Solati et al., 2018), and Alzheimer's disease (Gamba et al., 2015). Moreover, elevations in pro-inflammatory bioactive lipid species may help to explain the angiogenic behavioural effects (Chiurchiù & Maccarrone, 2016) of FTY720 reported here in young mice (Figure 3a–f). The lipids PCOH 39:10 (1.59-fold increase) and PCOH 41:10 (1.92-fold increase) also demonstrated apparent dose-dependent elevations in response to FTY720 treatment (Figure 9a,b). Although oxidised lipids can induce inflammation, it has also been shown that oxidised lipids are potent inhibitors of toll-like receptor-4 (TLR4)-mediated inflammatory signalling cascades (Oskolkova et al., 2010). Therefore, at low concentrations, oxidised lipids may act to inhibit lipopolysaccharide (LPS)-induced up-regulation of pro-inflammatory cytokine release from cells. Indeed, we have previously shown that FTY720 inhibits LPS-induced LIX chemokine (CXCL5) release from astrocytes and microglia (O'Sullivan et al., 2018) and can decrease the release of LIX, MIP-1 α , and MIP-3 α from cerebellar slice cultures exposed to the demyelinating agent, lysolecithin (Sheridan

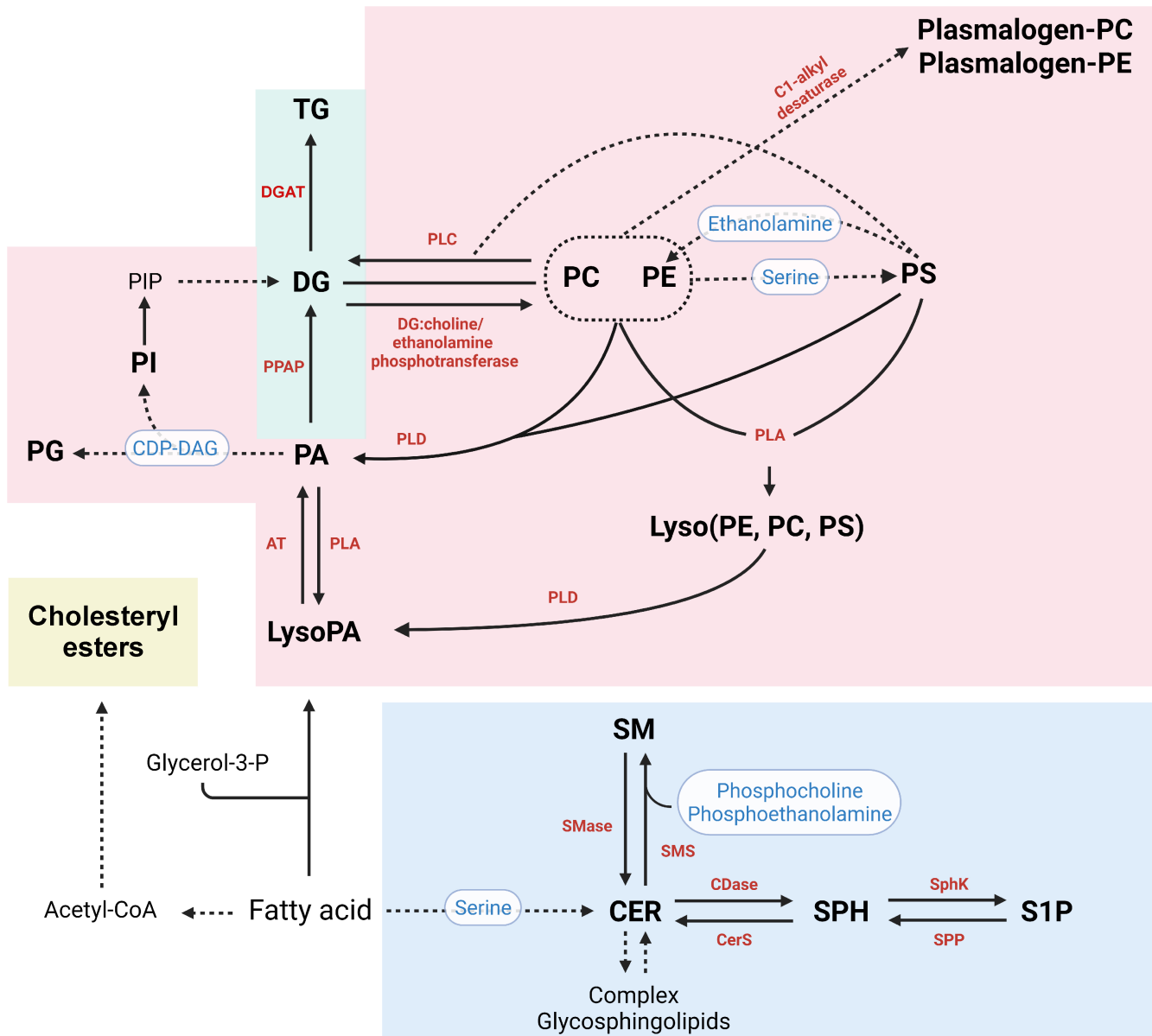


FIGURE 10 Mechanisms of lipid synthesis and metabolism in mammalian cells. Schematic overview of the pathways involved in the synthesis of glycerophospholipids (background in light red), glycerolipids (background in green), sphingolipids (background in blue), and sterol lipids (background in yellow). Saturated and unsaturated FAs are combined with glycerol-3-phosphate (glycerol-3-P) to produce glycerophospholipids and glycerolipids. Cholesteryl esters are formed through a multi-step enzymatic biosynthetic process that begins with acetyl-CoA. Enzymes involved in the multiple lipid synthesis pathways shown are indicated in red. The dashed arrows signify indirect pathways. Molecules in blue represent the products required to synthesise the lipids shown. Enzyme abbreviations: AT, 1-acylglycerol-3-phosphate O-acyltransferase; CDase ceramidase; CerS, ceramide synthase; DGAT, diacylglycerol O-acyltransferase; PLA, phospholipase A; PLC, phospholipase C; PLD, phospholipase D; PPAP, phosphatidic acid phosphatase; SMase, sphingomyelinase; SMS, sphingomyelin synthase; SphK, sphingosine kinase; SPP, sphingosine 1-phosphate phosphatase; CDase ceramidase; SphK, sphingosine kinase. Metabolite abbreviations: CDP-DAG, cytidine diphosphate diacylglycerol; CER, ceramide; DG, diacylglycerol; PA, phosphatidic acid; PC, phosphatidylcholine; PE, phosphatidylethanolamine; PG, phosphatidylglycerol; PI, phosphatidylinositol; PIP, phosphatidylinositol phosphate; PS, phosphatidylserine; S1P, sphingosine 1-phosphate; SM, sphingomyelin; SPH, sphingosine; TG, triacylglycerol. Figure created using [BioRender.com](https://www.biorender.com).

& Dev, 2012). Another observation with potential functional significance was that 7 of the 17 lipid species that demonstrated FTY720-mediated elevations between 1.5-fold and 1.9-fold above control levels belonged to the sphingomyelin (SM) class (Table S1). SMs can suppress oxidised phosphatidylcholine-mediated increases

in phospholipase A2 (PLA2) enzyme activity in a dose-dependent manner (Korotaeva et al., 2010), which may explain FTY720's ability to inhibit PLA2 (Payne et al., 2007) and reduce inflammation. Moreover, the lipids SM d35:2 (1.5-fold increase) and SM d32:1 (1.64-fold increase) also demonstrated dose-dependent elevations



in response to chronic FTY720 exposure (Figure 9n,o), highlighting their potentially important roles in FTY720's mechanism of action in the brain.

Interestingly, 8 out of the top 25 most abundant lipid species identified in the mouse hippocampus were increased following chronic FTY720 treatment. Five of these lipids belonged to the phosphatidylethanolamine (PE) lipid class (PE 18:0_20:4; PE 18:0_22:6; PE 16:0_22:6; PE 18:1_18:0; and PE 16:0_20:4), and three belonged to the plasmenyl-PE lipid class (plasmenyl-PE 18:0_22:6; plasmenyl-PE 18:0_22:4; and plasmenyl-PE 16:0_22:4). PE is located on the inner leaflet of the plasma membrane (Fadell & Xue, 2009), and an increase in this class of glycerophospholipid can lead to enhanced membrane fluidity and facilitate formation and fusion of vesicles with the synaptic membrane, thus regulating neurotransmission (Glaser & Gross, 1995; Lohner, 1996). In total, 23 distinct phosphatidylethanolamine lipid species were up-regulated in the hippocampus of FTY720-treated mice, with PE 18:0_22:5 showing the highest fold change of 1.59 times above control animals. Plasmalogens are also abundant in the brain, and these glycerophospholipids are located in the cell membranes of all CNS cell types (Fitzner et al., 2020; Koch et al., 2020). We identified 101 distinct plasmalogens in our hippocampal tissue samples, and the plasmenyl-PE lipids were, by far, the most concentrated class of plasmalogens (49 species in total) in the hippocampus. Moreover, plasmenyl-PE lipids were the only lipid class to demonstrate a significant up-regulation following FTY720 exposure (Figure 8f). They are known to be important for the assembly and stability of microdomains in lipid rafts and in cholesterol-rich regions of the cell membrane. Plasmenyl-PE lipids contain a vinyl-ether and an ester bond in glycerol backbone sn-1 and sn-2 positions, respectively (Messias et al., 2018), unlike other glycerophospholipids. Plasmalogens also tend to form tightly packed membranes, which may be attributed to the highly ordered state of the sn1 chain and the close packing of sn1 and sn2 chains (Han & Gross, 1990; Rog & Koivuniemi, 2016). Therefore, the physicochemical properties of cell membranes, their rigidity, and the bilayer thickness may all be regulated by changes in the concentration and the distribution of plasmalogens (Rog & Koivuniemi, 2016). Importantly, plasmalogens can protect lipid bilayers against the damaging effects of oxidation by scavenger radicals, such as ROS and reactive nitrogen species. As such, decreased plasmalogen concentrations may increase one's susceptibility to developing neurodegenerative or neuroinflammatory disorders, such as Alzheimer's disease (Azad et al., 2021; Han et al., 2001), Parkinson's disease, or MS (Ferreira et al., 2021; Mawatari et al., 2020). Here, we demonstrate that FTY720 increases plasmenyl-PE levels from 17.0% to 20.5% of the total lipid composition of the mouse hippocampus, which may increase the resistance of vulnerable neurons to oxidative stress (Zoeller et al., 2002) and explain why other studies have found that FTY720 can reverse cognitive deficits in animal models of CNS diseases (Fagan et al., 2022; Udagawa & Hino, 2022).

The only lipid class we found to be down-regulated in the mouse hippocampus following 3 weeks of FTY720 exposure was phosphatidic acid (PA; Figure 8l). PA is a low-abundant membrane

phospholipid (ca. 1% of the total lipid composition of the hippocampus). However, PA constitutes the original building block from which most glycerophospholipids are synthesised and, therefore, plays pertinent roles in membrane structure and function, as well as acting as a recruiter and activator of other lipid signalling molecules (Tanguy et al., 2019). PA exhibits a cone-shaped geometry allowing it to alter cell membrane topology and reducing the energy barrier for membrane bending, thus acting as a fusogenic lipid (Bills & Knowles, 2022; Kooijman et al., 2003). A decrease in PA lipids could be an indirect clue that phospholipase D (PLD)-dependent pathways are down-regulated (Figure 10). PLD catalyses the hydrolysis of phosphatidylcholine (PC) into PA and free choline. Interestingly, oligomeric A β can enhance PLD activity in cultured neurons (Oliveira et al., 2010), and so decreasing PLD activity (and consequently PA expression) may exert a neuroprotective effect in the hippocampus. However, one must be cautious not to overinterpret the observations presented here in this study, particularly given that results are derived from the brains of young healthy mice.

4.3 | Role of sphingolipids in the mechanism of action of FTY720 in the brain

Of the 99 lipids that were found to be increased in the mouse hippocampus following FTY720 exposure, 17 lipid species displayed dose-dependent regulation in their expression levels (Figure 9). Four of these lipids belonged to the sphingomyelin class of lipids. Three of them (SM d32:1; SM d35:2; and SM d43:1) displayed dose-dependent increases in expression with increasing FTY720 levels. Interestingly, although SM d36:0 levels were elevated above control values (fold change = 1.36; $-\text{Log}_{10}(p\text{-value}) = 4.35$), this particular lipid species demonstrated a dose-dependent decrease in expression, that is, the higher the concentration of FTY720, the lower the concentration of SM d36:0, but only in drug-treated mice since FTY720 levels were effectively zero in vehicle control animals. Sphingomyelin (SM) is an important component of the plasma membrane of CNS cells (Levade et al., 1999) and is highly expressed in the myelin sheath of neuronal axons (Babin et al., 1993). As discussed above, FTY720 can inhibit the activity of acid SMase and decrease the conversion of sphingomyelins to ceramide (Dawson & Qin, 2011), thus enhancing the expression of sphingomyelin (SM) lipid species (Crivelli et al., 2022). Limiting the conversion of SM lipids to ceramide can prevent apoptotic signalling cascades from being activated in the cell and may protect vulnerable neurons from degeneration or demyelination. Indeed, SMase has been investigated as a therapeutic target for the treatment of Alzheimer's disease (Park et al., 2022), since overactivity of this ceramide-producing enzyme is implicated in several neuropathologies (Jana et al., 2009; Lee et al., 2014; Mielke et al., 2013; Ong et al., 2015; van Doorn et al., 2012). Interestingly, the antidepressant, fluoxetine, has been shown to increase sphingomyelin levels by inactivating acid SMase (Kornhuber & Gulbins, 2021), a potential explanation as to why FTY720 may demonstrate antidepressant mechanisms of action under certain conditions. Although



our data show an up-regulation in several sphingomyelin lipid species, we are unable to confirm whether there are alterations in any other lipid classes involved in the SM synthesis pathway, including S1P or ceramide, which are precursors of sphingomyelin lipids. The absence of quantitative data regarding FTY720-mediated changes in ceramide or S1P is a key limitation of this study. Future work should focus on how the fatty acid chain length, the degree of saturation, and the relative concentrations of other sphingolipids are altered in the hippocampus in response to chronic FTY720 exposure.

SUMMARY

We present here a comprehensive overview of the lipidomic signature of the 6-week-old mouse hippocampus and the lipid species that are altered because of chronic treatment with the immune-modulating drug, FTY720. To our knowledge, this is the first detailed account of how FTY720 impacts the expression of structural and functional lipid species in a particular brain region, which is known to be important for learning, memory, and the processing of sensory and emotional stimuli. It is important to bear in mind that this is an exploratory study and many of the discussion points raised regarding the potential functional consequences of FTY720-mediated changes to brain lipids are at this point speculative in nature and require further investigation. However, this study has clinical relevance given the approval of FTY720 for children and adolescents above the age of 10 years, at a stage when the brain is still maturing and myelination continues. It is important to understand the full spectrum of molecular mechanisms that lipophilic drugs with long half-lives exert on the body's organs and tissues, including their therapeutic effects, non-therapeutic actions, and side-effect profiles. Such data will aid in the refinement of pharmacological treatment regimens and minimise the unwanted effects of disease-modifying drugs that otherwise help to improve the lives of people living with currently incurable autoimmune diseases of the central nervous system.

AUTHOR CONTRIBUTIONS

Daniela M. Magalhães: Data curation; formal analysis; funding acquisition; investigation; methodology; writing – review and editing. **Nicolas A. Stewart:** Investigation; methodology; resources; validation; writing – review and editing. **Myrthe Mampay:** Investigation; methodology. **Sara O. Rolle:** Formal analysis; validation. **Chloe M. Hall:** Formal analysis; validation. **Emad Moeendarbary:** Funding acquisition; supervision. **Melanie S. Flint:** Project administration; resources; supervision. **Ana M. Sebastião:** Resources; supervision. **Cláudia A. Valente:** Project administration; resources; supervision. **Marcus K. Dymond:** Data curation; formal analysis; investigation; methodology; project administration; resources; supervision; validation; writing – review and editing. **Graham K. Sheridan:** Conceptualization; data curation; formal analysis; funding acquisition; investigation; methodology; project administration; resources; supervision; validation; visualization; writing – original draft; writing – review and editing.

ACKNOWLEDGEMENTS

All experiments were conducted in compliance with the ARRIVE guidelines.

FUNDING INFORMATION

This work was supported by a Fundação para a Ciência e a Tecnologia (FCT) PhD scholarship to D.M. (PD/BD/128405/2017). Authors G.K.S. and E.M. are grateful for financial support from the Leverhulme Trust (RPG-2018-443).

CONFLICT OF INTEREST STATEMENT

Ana M. Sebastião is a handling editor for the Journal of Neurochemistry. The authors declare no other conflicts of interest and no competing financial interests.

DATA AVAILABILITY STATEMENT

The data that support the findings of this study are available from the corresponding author upon reasonable request.

ORCID

Daniela M. Magalhães <https://orcid.org/0000-0002-1662-2002>

Graham K. Sheridan <https://orcid.org/0000-0002-8493-2651>

REFERENCES

- Antony, B., Vanni, S., Shindou, H., & Ferreira, T. (2015). From zero to six double bonds: Phospholipid unsaturation and organelle function. *Trends in Cell Biology*, 25(7), 427–436. <https://doi.org/10.1016/j.tcb.2015.03.004>
- Asle-Rousta, M., Kolahdooz, Z., Oryan, S., Ahmadiani, A., & Dargahi, L. (2013). FTY720 (fingolimod) attenuates beta-amyloid peptide (A β 42)-induced impairment of spatial learning and memory in rats. *Journal of Molecular Neuroscience: MN*, 50(3), 524–532. <https://doi.org/10.1007/s12031-013-9979-6>
- Aureli, M., Grassi, S., Prioni, S., Sonnino, S., & Prinetti, A. (2015). Lipid membrane domains in the brain. *Biochimica et Biophysica Acta*, 1851(8), 1006–1016. <https://doi.org/10.1016/j.bbali.2015.02.001>
- Azad, A. K., Sheikh, A. M., Haque, M. A., Osago, H., Sakai, H., Shibby, A. Z., Yano, S., Michikawa, M., Hossain, S., Tabassum, S. A. G., Zhou, X., Zhang, Y., & Nagai, A. (2021). Time-dependent analysis of plasmalogens in the hippocampus of an Alzheimer's disease mouse model: A role of ethanolamine plasmalogen. *Brain Sciences*, 11(12), 1603. <https://doi.org/10.3390/brainsci11121603>
- Babin, F., Sarda, P., Limasset, B., Descomps, B., Rieu, D., Mendy, F., & Crastes de Paulet, A. (1993). Nervonic acid in red blood cell sphingomyelin in premature infants: An index of myelin maturation? *Lipids*, 28(7), 627–630. <https://doi.org/10.1007/BF02536057>
- Bahja, J., Stewart, N. A., & Dymond, M. K. (2022). Oxidative stress is inhibited by plant-based supplements: A quantitative lipidomic analysis of antioxidant activity and lipid compositional change. *Advances in Redox Research*, 6, 100054. <https://doi.org/10.1016/j.arres.2022.100054>
- Bailey, S. A., Zidell, R. H., & Perry, R. W. (2004). Relationships between organ weight and body/brain weight in the rat: What is the best analytical endpoint? *Toxicologic Pathology*, 32(4), 448–466. <https://doi.org/10.1080/01926230490465874>
- Bandhuvula, P., Tam, Y. Y., Oskouian, B., & Saba, J. D. (2005). The immune modulator FTY720 inhibits sphingosine-1-phosphate lyase activity. *The Journal of Biological Chemistry*, 280(40), 33697–33700. <https://doi.org/10.1074/jbc.C500294200>



- Barber, C. N., & Raben, D. M. (2019). Lipid metabolism crosstalk in the brain: Glia and neurons. *Frontiers in Cellular Neuroscience*, 13, 212. <https://doi.org/10.3389/fncel.2019.00212>
- Bates, D., Mächler, M., Bolker, B., & Walker, S. (2015). Fitting linear mixed-effects models using lme4. *Journal of Statistical Software*, 67(1), 1–48. <https://doi.org/10.18637/jss.v067.i01>
- Bills, B. L., & Knowles, M. K. (2022). Phosphatidic acid accumulates at areas of curvature in Tubulated lipid bilayers and liposomes. *Biomolecules*, 12(11), 1707. <https://doi.org/10.3390/biom12111707>
- Bligh, E. G., & Dyer, W. J. (1959). A rapid method of total lipid extraction and purification. *Canadian Journal of Biochemistry and Physiology*, 37(8), 911–917. <https://doi.org/10.1139/o59-099>
- Blusztajn, J. K., Liscovitch, M., Mauron, C., Richardson, U. I., & Wurtman, R. J. (1987). Phosphatidylcholine as a precursor of choline for acetylcholine synthesis. *Journal of Neural Transmission. Supplementum*, 24, 247–259.
- Breslow, D. K., & Weissman, J. S. (2010). Membranes in balance: Mechanisms of sphingolipid homeostasis. *Molecular Cell*, 40(2), 267–279. <https://doi.org/10.1016/j.molcel.2010.10.005>
- Brinkmann, V. (2007). Sphingosine 1-phosphate receptors in health and disease: Mechanistic insights from gene deletion studies and reverse pharmacology. *Pharmacology & Therapeutics*, 115(1), 84–105. <https://doi.org/10.1016/j.pharmthera.2007.04.006>
- Brinkmann, V., Billich, A., Baumruker, T., Heining, P., Schmouder, R., Francis, G., Aradhye, S., & Burtin, P. (2010). Fingolimod (FTY720): Discovery and development of an oral drug to treat multiple sclerosis. *Nature Reviews. Drug Discovery*, 9(11), 883–897. <https://doi.org/10.1038/nrd3248>
- Brinkmann, V., Cyster, J. G., & Hla, T. (2004). FTY720: Sphingosine 1-phosphate receptor-1 in the control of lymphocyte egress and endothelial barrier function. *American Journal of Transplantation: Official Journal of the American Society of Transplantation and the American Society of Transplant Surgeons*, 4(7), 1019–1025. <https://doi.org/10.1111/j.1600-6143.2004.00476.x>
- Caires, R., Sierra-Valdez, F. J., Millet, J. R. M., Herwig, J. D., Roan, E., Vásquez, V., & Cordero-Morales, J. F. (2017). Omega-3 fatty acids modulate TRPV4 function through plasma membrane remodeling. *Cell Reports*, 21(1), 246–258. <https://doi.org/10.1016/j.celrep.2017.09.029>
- Carta, M., Lanore, F., Rebola, N., Szabo, Z., Da Silva, S. V., Lourenço, J., Verraes, A., Nadler, A., Schultz, C., Blanchet, C., & Mulle, C. (2014). Membrane lipids tune synaptic transmission by direct modulation of presynaptic potassium channels. *Neuron*, 81(4), 787–799. <https://doi.org/10.1016/j.neuron.2013.12.028>
- Chang, C. Y., Ke, D. S., & Chen, J. Y. (2009). Essential fatty acids and human brain. *Acta Neurologica Taiwanica*, 18(4), 231–241.
- Chang, M., Binder, C. J., Torzewski, M., & Witztum, J. L. (2002). C-reactive protein binds to both oxidized LDL and apoptotic cells through recognition of a common ligand: Phosphorylcholine of oxidized phospholipids. *Proceedings of the National Academy of Sciences of the United States of America*, 99(20), 13043–13048. <https://doi.org/10.1073/pnas.192399699>
- Chen, H., Tran, J. A., Eckerd, A., Huynh, T. P., Elliott, M. H., Brush, R. S., & Mandal, N. A. (2013). Inhibition of de novo ceramide biosynthesis by FTY720 protects rat retina from light-induced degeneration. *Journal of Lipid Research*, 54(6), 1616–1629. <https://doi.org/10.1194/jlr.M035048>
- Chiba, K., Kataoka, H., Seki, N., Shimano, K., Koyama, M., Fukunari, A., Sugahara, K., & Sugita, T. (2011). Fingolimod (FTY720), sphingosine 1-phosphate receptor modulator, shows superior efficacy as compared with interferon- β in mouse experimental autoimmune encephalomyelitis. *International Immunopharmacology*, 11(3), 366–372. <https://doi.org/10.1016/j.intimp.2010.10.005>
- Chiurchiù, V., & Maccarrone, M. (2016). Bioactive lipids as modulators of immunity, inflammation and emotions. *Current Opinion in Pharmacology*, 29, 54–62. <https://doi.org/10.1016/j.coph.2016.06.005>
- Choleris, E., Thomas, A. W., Kavaliers, M., & Prato, F. S. (2001). A detailed ethological analysis of the mouse open field test: Effects of diazepam, chlordiazepoxide and an extremely low frequency pulsed magnetic field. *Neuroscience and Biobehavioral Reviews*, 25(3), 235–260. [https://doi.org/10.1016/s0149-7634\(01\)00011-2](https://doi.org/10.1016/s0149-7634(01)00011-2)
- Comi, G., Patti, F., Rocca, M. A., Mattioli, F. C., Amato, M. P., Gallo, P., Centonze, D., Pozzilli, C., Saccà, F., Bergh, F. T., Bartezaghi, M., Turrini, R., Filippi, M., & Golden Study Group. (2017). Efficacy of fingolimod and interferon beta-1b on cognitive, MRI, and clinical outcomes in relapsing-remitting multiple sclerosis: An 18-month, open-label, rater-blinded, randomised, multicentre study (the GOLDEN study). *Journal of Neurology*, 264(12), 2436–2449. <https://doi.org/10.1007/s00415-017-8642-5>
- Cordero-Morales, J. F., & Vásquez, V. (2018). How lipids contribute to Ion Channel function, a fat perspective on direct and indirect interactions. *Current Opinion in Structural Biology*, 51, 92–98. <https://doi.org/10.1016/j.sbi.2018.03.015>
- Crivelli, S. M., Luo, Q., Kruining, D. V., Giovagnoni, C., Mané-Damas, M., den Hoedt, S., Berkes, D., De Vries, H. E., Mulder, M. T., Walter, J., Waelkens, E., Derua, R., Swinnen, J. V., Dehairs, J., Wijndans, E. P. M., Bieberich, E., Losen, M., & Martinez-Martinez, P. (2022). FTY720 decreases ceramides levels in the brain and prevents memory impairments in a mouse model of familial Alzheimer's disease expressing APOE4. *Biomedicine & Pharmacotherapy = Biomedecine & Pharmacotherapie*, 152, 113240. <https://doi.org/10.1016/j.biopha.2022.113240>
- Cuvillier, O., Pirianov, G., Kleuser, B., Vanek, P. G., Coso, O. A., Gutkind, S., & Spiegel, S. (1996). Suppression of ceramide-mediated programmed cell death by sphingosine-1-phosphate. *Nature*, 381(6585), 800–803. <https://doi.org/10.1038/381800a0>
- David, O. J., Kovarik, J. M., & Schmouder, R. L. (2012). Clinical pharmacokinetics of fingolimod. *Clinical Pharmacokinetics*, 51(1), 15–28. <https://doi.org/10.2165/11596550-000000000-00000>
- Dawson, G., & Qin, J. (2011). Gilenya (FTY720) inhibits acid sphingomyelinase by a mechanism similar to tricyclic antidepressants. *Biochemical and Biophysical Research Communications*, 404(1), 321–323. <https://doi.org/10.1016/j.bbrc.2010.11.115>
- de Bruin, N. M., Schmitz, K., Schiffmann, S., Tafferner, N., Schmidt, M., Jordan, H., Häßler, A., Tegeder, I., Geisslinger, G., & Parnham, M. J. (2016). Multiple rodent models and behavioral measures reveal unexpected responses to FTY720 and DMF in experimental autoimmune encephalomyelitis. *Behavioural Brain Research*, 300, 160–174. <https://doi.org/10.1016/j.bbr.2015.12.006>
- Dev, K. K., Mullershausen, F., Mattes, H., Kuhn, R. R., Bilbe, G., Hoyer, D., & Mir, A. (2008). Brain sphingosine-1-phosphate receptors: Implication for FTY720 in the treatment of multiple sclerosis. *Pharmacology & Therapeutics*, 117(1), 77–93. <https://doi.org/10.1016/j.pharmthera.2007.08.005>
- Di Menna, L., Molinaro, G., Di Nuzzo, L., Rizzo, B., Zappulla, C., Pozzilli, C., Turrini, R., Caraci, F., Copani, A., Battaglia, G., Nicoletti, F., & Bruno, V. (2013). Fingolimod protects cultured cortical neurons against excitotoxic death. *Pharmacological Research*, 67(1), 1–9. <https://doi.org/10.1016/j.phrs.2012.10.004>
- di Nuzzo, L., Orlando, R., Tognoli, C., Di Pietro, P., Bertini, G., Miele, J., Bucci, D., Motolese, M., Scaccianoce, S., Caruso, A., Mauro, G., De Lucia, C., Battaglia, G., Bruno, V., Fabene, P. F., & Nicoletti, F. (2015). Antidepressant activity of fingolimod in mice. *Pharmacology Research & Perspectives*, 3(3), e00135. <https://doi.org/10.1002/prp2.135>
- Dos Santos, N., Novaes, L. S., Dragunas, G., Rodrigues, J. R., Brandão, W., Camarini, R., Peron, J. P. S., & Munhoz, C. D. (2019). High dose of dexamethasone protects against EAE-induced motor deficits but impairs learning/memory in C57BL/6 mice. *Scientific Reports*, 9(1), 6673. <https://doi.org/10.1038/s41598-019-43217-3>
- Dymond, M. K. (2021). Lipid monolayer spontaneous curvatures: A collection of published values. *Chemistry and Physics of Lipids*, 239, 105117. <https://doi.org/10.1016/j.chemphyslip.2021.105117>



- Ebert, D., Haller, R. G., & Walton, M. E. (2003). Energy contribution of octanoate to intact rat brain metabolism measured by ^{13}C nuclear magnetic resonance spectroscopy. *The Journal of Neuroscience: The Official Journal of the Society for Neuroscience*, 23(13), 5928–5935. <https://doi.org/10.1523/JNEUROSCI.23-13-05928.2003>
- Fadeel, B., & Xue, D. (2009). The ins and outs of phospholipid asymmetry in the plasma membrane: Roles in health and disease. *Critical Reviews in Biochemistry and Molecular Biology*, 44(5), 264–277. <https://doi.org/10.1080/10409230903193307>
- Fagan, S. G., Bechet, S., & Dev, K. K. (2022). Fingolimod rescues memory and improves pathological hallmarks in the 3xTg-AD model of Alzheimer's disease. *Molecular Neurobiology*, 59(3), 1882–1895. <https://doi.org/10.1007/s12035-021-02613-5>
- Fanselow, M. S., & Dong, H. W. (2010). Are the dorsal and ventral hippocampus functionally distinct structures? *Neuron*, 65(1), 7–19. <https://doi.org/10.1016/j.neuron.2009.11.031>
- Ferbinteanu, J., & McDonald, R. J. (2001). Dorsal/ventral hippocampus, fornix, and conditioned place preference. *Hippocampus*, 11(2), 187–200. <https://doi.org/10.1002/hipo.1036>
- Ferreira, H. B., Melo, T., Monteiro, A., Paiva, A., Domingues, P., & Domingues, M. R. (2021). Serum phospholipidomics reveals altered lipid profile and promising biomarkers in multiple sclerosis. *Archives of Biochemistry and Biophysics*, 697, 108672. <https://doi.org/10.1016/j.abb.2020.108672>
- Fitzner, D., Bader, J. M., Penkert, H., Bergner, C. G., Su, M., Weil, M. T., Surma, M. A., Mann, M., Klose, C., & Simons, M. (2020). Cell-type- and brain-region-resolved mouse brain lipidome. *Cell Reports*, 32(11), 108132. <https://doi.org/10.1016/j.celrep.2020.108132>
- Fonseca, J. (2015). Fingolimod real world experience: Efficacy and safety in clinical practice. *Neuroscience Journal*, 2015, 389360. <https://doi.org/10.1155/2015/389360>
- Foster, C. A., Howard, L. M., Schweitzer, A., Persohn, E., Hiestand, P. C., Balatoni, B., Reuschel, R., Beerli, C., Schwartz, M., & Billich, A. (2007). Brain penetration of the oral immunomodulatory drug FTY720 and its phosphorylation in the central nervous system during experimental autoimmune encephalomyelitis: Consequences for mode of action in multiple sclerosis. *The Journal of Pharmacology and Experimental Therapeutics*, 323(2), 469–475. <https://doi.org/10.1124/jpet.107.127183>
- Fukumoto, K., Mizoguchi, H., Takeuchi, H., Horiuchi, H., Kawanokuchi, J., Jin, S., Mizuno, T., & Suzumura, A. (2014). Fingolimod increases brain-derived neurotrophic factor levels and ameliorates amyloid β -induced memory impairment. *Behavioural Brain Research*, 268, 88–93. <https://doi.org/10.1016/j.bbr.2014.03.046>
- Gamba, P., Testa, G., Gargiulo, S., Staurengi, E., Poli, G., & Leonarduzzi, G. (2015). Oxidized cholesterol as the driving force behind the development of Alzheimer's disease. *Frontiers in Aging Neuroscience*, 7, 119. <https://doi.org/10.3389/fnagi.2015.00119>
- Gault, C. R., Obeid, L. M., & Hannun, Y. A. (2010). An overview of sphingolipid metabolism: From synthesis to breakdown. *Advances in Experimental Medicine and Biology*, 688, 1–23. https://doi.org/10.1007/978-1-4419-6741-1_1
- Gauster, M., Rechberger, G., Sovic, A., Hörl, G., Steyrer, E., Sattler, W., & Frank, S. (2005). Endothelial lipase releases saturated and unsaturated fatty acids of high density lipoprotein phosphatidylcholine. *Journal of Lipid Research*, 46(7), 1517–1525. <https://doi.org/10.1194/jlr.M500054-JLR200>
- Gawrisch, K., & Soubias, O. (2008). Structure and dynamics of polyunsaturated hydrocarbon chains in lipid bilayers-significance for GPCR function. *Chemistry and Physics of Lipids*, 153(1), 64–75. <https://doi.org/10.1016/j.chemphyslip.2008.02.016>
- Ghasemi-Kasman, M., Nosratiyan, N., Hashemian, M., Ahmadian, S. R., Parsian, H., & Rostami-Mansoor, S. (2022). Intranasal administration of fingolimod (FTY720) attenuates demyelination area in lysocleithin-induced demyelination model of rat optic chiasm. *Multiple Sclerosis and Related Disorders*, 59, 103518. <https://doi.org/10.1016/j.msard.2022.103518>
- Glaser, P. E., & Gross, R. W. (1995). Rapid plasmeneethanolamine-selective fusion of membrane bilayers catalyzed by an isoform of glyceraldehyde-3-phosphate dehydrogenase: Discrimination between glycolytic and fusogenic roles of individual isoforms. *Biochemistry*, 34(38), 12193–12203. <https://doi.org/10.1021/bi00038a013>
- Gräler, M. H., & Goetzl, E. J. (2004). The immunosuppressant FTY720 down-regulates sphingosine 1-phosphate G-protein-coupled receptors. *FASEB Journal: Official Publication of the Federation of American Societies for Experimental Biology*, 18(3), 551–553. <https://doi.org/10.1096/fj.03-0910fje>
- Grassi, S., Mauri, L., Prioni, S., Cabitta, L., Sonnino, S., Prinetti, A., & Giussani, P. (2019). Sphingosine 1-phosphate receptors and metabolic enzymes as druggable targets for brain diseases. *Frontiers in Pharmacology*, 10, 807. <https://doi.org/10.3389/fphar.2019.00807>
- Groves, A., Kihara, Y., & Chun, J. (2013). Fingolimod: Direct CNS effects of sphingosine 1-phosphate (S1P) receptor modulation and implications in multiple sclerosis therapy. *Journal of the Neurological Sciences*, 328(1–2), 9–18. <https://doi.org/10.1016/j.jns.2013.02.011>
- Guo, Y., Gan, X., Zhou, H., Zhou, H., Pu, S., Long, X., Ren, C., Feng, T., & Tang, H. (2020). Fingolimod suppressed the chronic unpredictable mild stress-induced depressive-like behaviors via affecting microglial and NLRP3 inflammasome activation. *Life Sciences*, 263, 118582. <https://doi.org/10.1016/j.lfs.2020.118582>
- Hagihara, K., Kanda, Y., Ishida, K., Satoh, R., Takasaki, T., Maeda, T., & Sugiura, R. (2020). Chemical genetic analysis of FTY720- and Ca^{2+} -sensitive mutants reveals a functional connection between FTY720 and membrane trafficking. *Genes to Cells: Devoted to Molecular & Cellular Mechanisms*, 25(9), 637–645. <https://doi.org/10.1111/gtc.12800>
- Hait, N. C., Oskeritzian, C. A., Paugh, S. W., Milstien, S., & Spiegel, S. (2006). Sphingosine kinases, sphingosine 1-phosphate, apoptosis and diseases. *Biochimica et Biophysica Acta*, 1758(12), 2016–2026. <https://doi.org/10.1016/j.bbamem.2006.08.007>
- Hait, N. C., Wise, L. E., Allegood, J. C., O'Brien, M., Avni, D., Reeves, T. M., Knapp, P. E., Lu, J., Luo, C., Miles, M. F., Milstien, S., Lichtman, A. H., & Spiegel, S. (2014). Active, phosphorylated fingolimod inhibits histone deacetylases and facilitates fear extinction memory. *Nature Neuroscience*, 17(7), 971–980. <https://doi.org/10.1038/nn.3728>
- Hammelrath, L., Škokić, S., Khmelinskii, A., Hess, A., van der Knaap, N., Staring, M., Lelieveldt, B. P. F., Wiedermann, D., & Hoehn, M. (2016). Morphological maturation of the mouse brain: An in vivo MRI and histology investigation. *NeuroImage*, 125, 144–152. <https://doi.org/10.1016/j.neuroimage.2015.10.009>
- Han, X., Holtzman, D. M., & McKeel, D. W., Jr. (2001). Plasmalogen deficiency in early Alzheimer's disease subjects and in animal models: Molecular characterization using electrospray ionization mass spectrometry. *Journal of Neurochemistry*, 77(4), 1168–1180. <https://doi.org/10.1046/j.1471-4159.2001.00332.x>
- Han, X. L., & Gross, R. W. (1990). Plasmeneethanolamine and phosphatidylcholine membrane bilayers possess distinct conformational motifs. *Biochemistry*, 29(20), 4992–4996. <https://doi.org/10.1021/bi00472a032>
- Hanada, M., Sugiura, Y., Shinjo, R., Masaki, N., Imagama, S., Ishiguro, N., Matsuyama, Y., & Setou, M. (2012). Spatiotemporal alteration of phospholipids and prostaglandins in a rat model of spinal cord injury. *Analytical and Bioanalytical Chemistry*, 403(7), 1873–1884. <https://doi.org/10.1007/s00216-012-5900-3>
- Henke, P. G. (1990). Hippocampal pathway to the amygdala and stress ulcer development. *Brain Research Bulletin*, 25(5), 691–695. [https://doi.org/10.1016/0361-9230\(90\)90044-z](https://doi.org/10.1016/0361-9230(90)90044-z)
- Hunter, S. F., Bowen, J. D., & Reder, A. T. (2016). The direct effects of Fingolimod in the central nervous system: Implications for relapsing

- multiple sclerosis. *CNS Drugs*, 30(2), 135–147. <https://doi.org/10.1007/s40263-015-0297-0>
- Hutchins, P. D., Russell, J. D., & Coon, J. J. (2018). LipiDex: An integrated software package for high-confidence lipid identification. *Cell Systems*, 6(5), 621–625.e5. <https://doi.org/10.1016/j.cels.2018.03.011>
- Jaillard, C., Harrison, S., Stankoff, B., Aigrot, M. S., Calver, A. R., Duddy, G., Walsh, F. S., Pangalos, M. N., Arimura, N., Kaibuchi, K., Zalc, B., & Lubetzki, C. (2005). Edg8/S1P5: An oligodendroglial receptor with dual function on process retraction and cell survival. *The Journal of Neuroscience: The Official Journal of the Society for Neuroscience*, 25(6), 1459–1469. <https://doi.org/10.1523/JNEUROSCI.4645-04.2005>
- Jana, A., Hogan, E. L., & Pahan, K. (2009). Ceramide and neurodegeneration: Susceptibility of neurons and oligodendrocytes to cell damage and death. *Journal of the Neurological Sciences*, 278(1–2), 5–15. <https://doi.org/10.1016/j.jns.2008.12.010>
- Jęśko, H., Wencel, P. L., Wójtowicz, S., Strosznajder, J., Lukiw, W. J., & Strosznajder, R. P. (2020). Fingolimod affects transcription of genes encoding enzymes of ceramide metabolism in animal model of Alzheimer's disease. *Molecular Neurobiology*, 57(6), 2799–2811. <https://doi.org/10.1007/s12035-020-01908-3>
- Jiménez-Rojo, N., Sot, J., Viguera, A. R., Collado, M. I., Torrecillas, A., Gómez-Fernández, J. C., Goñi, F. M., & Alonso, A. (2014). Membrane permeabilization induced by sphingosine: Effect of negatively charged lipids. *Biophysical Journal*, 106(12), 2577–2584. <https://doi.org/10.1016/j.bpj.2014.04.038>
- Jobin, M.-L., De Smedt-Peyrusse, V., Ducrocq, F., Baccouch, R., Oummadi, A., Pedersen, M. H., Medel-Lacruz, B., Angelo, M.-F., Villette, S., Van Delft, P., Fouillen, L., Mongrand, S., Selent, J., Tolentino-Cortez, T., Barreda-Gómez, G., Grégoire, S., Masson, E., Durroux, T., Javitch, J. A., ... Trifilieff, P. (2023). Impact of membrane lipid polyunsaturation on dopamine D2 receptor ligand binding and signaling. *Molecular Psychiatry*, 1–10, 1960–1969. <https://doi.org/10.1038/s41380-022-01928-6>
- Kappos, L., O'Connor, P., Radue, E. W., Polman, C., Hohlfeld, R., Selmaj, K., Ritter, S., Schlosshauer, R., von Rosenstiel, P., Zhang-Auberson, L., & Francis, G. (2015). Long-term effects of fingolimod in multiple sclerosis: The randomized FREEDOMS extension trial. *Neurology*, 84(15), 1582–1591. <https://doi.org/10.1212/WNL.0000000000001462>
- Kartalou, G. I., Salgueiro-Pereira, A. R., Endres, T., Lesnikova, A., Casarotto, P., Pousinha, P., Delanoë, K., Edelmann, E., Castrén, E., Gottmann, K., Marie, H., & Lessmann, V. (2020). Anti-inflammatory treatment with FTY720 starting after onset of symptoms reverses synaptic deficits in an AD mouse model. *International Journal of Molecular Sciences*, 21(23), 8957. <https://doi.org/10.3390/ijms21238957>
- Katajamaa, M., Miettinen, J., & Oresic, M. (2006). MZmine: Toolbox for processing and visualization of mass spectrometry based molecular profile data. *Bioinformatics (Oxford, England)*, 22(5), 634–636. <https://doi.org/10.1093/bioinformatics/btk039>
- Kjelstrup, K. G., Tuvnes, F. A., Steffenach, H. A., Murison, R., Moser, E. I., & Moser, M. B. (2002). Reduced fear expression after lesions of the ventral hippocampus. *Proceedings of the National Academy of Sciences of the United States of America*, 99(16), 10825–10830. <https://doi.org/10.1073/pnas.152112399>
- Klur, S., Muller, C., Pereira de Vasconcelos, A., Ballard, T., Lopez, J., Galani, R., Certa, U., & Cassel, J. C. (2009). Hippocampal-dependent spatial memory functions might be lateralized in rats: An approach combining gene expression profiling and reversible inactivation. *Hippocampus*, 19(9), 800–816. <https://doi.org/10.1002/hipo.20562>
- Koch, J., Lackner, K., Wohlfarter, Y., Sailer, S., Zschocke, J., Werner, E. R., Watschinger, K., & Keller, M. A. (2020). Unequivocal mapping of molecular ether lipid species by LC-MS/MS in Plasmalogen-deficient mice. *Analytical Chemistry*, 92(16), 11268–11276. <https://doi.org/10.1021/acs.analchem.0c01933>
- Kocovski, P., Tabassum-Sheikh, N., Marinis, S., Dang, P. T., Hale, M. W., & Orian, J. M. (2021). Immunomodulation eliminates inflammation in the hippocampus in experimental autoimmune encephalomyelitis, but does not ameliorate anxiety-like behavior. *Frontiers in Immunology*, 12, 639650. <https://doi.org/10.3389/fimmu.2021.639650>
- Kooijman, E. E., Chupin, V., de Kruijff, B., & Burger, K. N. J. (2003). Modulation of membrane curvature by phosphatidic acid and lysophosphatidic acid. *Traffic*, 4(3), 162–174. <https://doi.org/10.1034/j.1600-0854.2003.00086.x>
- Kornhuber, J., & Gulbins, E. (2021). New molecular targets for antidepressant drugs. *Pharmaceuticals (Basel, Switzerland)*, 14(9), 894. <https://doi.org/10.3390/ph14090894>
- Korotaeva, A. A., Samoilo, E. V., Piksina, G. F., & Prokazova, N. V. (2010). Oxidized phosphatidylcholine stimulates activity of secretory phospholipase A2 group IIA and abolishes sphingomyelin-induced inhibition of the enzyme. *Prostaglandins & Other Lipid Mediators*, 91(1–2), 38–41. <https://doi.org/10.1016/j.prostaglandins.2009.12.004>
- Kumari, A. (2018). Chapter 13—ceramide structure and derivatives. In A. Kumari (Ed.), *Sweet biochemistry* (pp. 59–61). Academic Press.
- Lahiri, S., Park, H., Laviad, E. L., Lu, X., Bittman, R., & Futerman, A. H. (2009). Ceramide synthesis is modulated by the sphingosine analog FTY720 via a mixture of uncompetitive and noncompetitive inhibition in an acyl-CoA chain length-dependent manner. *The Journal of Biological Chemistry*, 284(24), 16090–16098. <https://doi.org/10.1074/jbc.M807438200>
- Langdon, D. W., Tomic, D., Penner, I. K., Calabrese, P., Cutter, G., Häring, D. A., Dahlke, F., & Kappos, L. (2021). Baseline characteristics and effects of fingolimod on cognitive performance in patients with relapsing-remitting multiple sclerosis. *European Journal of Neurology*, 28(12), 4135–4145. <https://doi.org/10.1111/ene.15081>
- Le Magueresse, C., & Monyer, H. (2013). GABAergic interneurons shape the functional maturation of the cortex. *Neuron*, 77(3), 388–405. <https://doi.org/10.1016/j.neuron.2013.01.011>
- Lee, A. G. (2004). How lipids affect the activities of integral membrane proteins. *Biochimica et Biophysica Acta*, 1666(1–2), 62–87. <https://doi.org/10.1016/j.bbamem.2004.05.012>
- Lee, J. K., Jin, H. K., Park, M. H., Kim, B. R., Lee, P. H., Nakauchi, H., Carter, J. E., He, X., Schuchman, E. H., & Bae, J. S. (2014). Acid sphingomyelinase modulates the autophagic process by controlling lysosomal biogenesis in Alzheimer's disease. *The Journal of Experimental Medicine*, 211(8), 1551–1570. <https://doi.org/10.1084/jem.20132451>
- Lei, E., Vacy, K., & Boon, W. C. (2016). Fatty acids and their therapeutic potential in neurological disorders. *Neurochemistry International*, 95, 75–84. <https://doi.org/10.1016/j.neuint.2016.02.014>
- Leung, J., Santo, T., Colledge-Frisby, S., Mekonen, T., Thomson, K., Degenhardt, L., Connor, J. P., Hall, W., & Stjepanović, D. (2022). Mood and anxiety symptoms in persons taking prescription opioids: A systematic review with meta-analyses of longitudinal studies. *Pain Medicine (Malden, Mass.)*, 23(8), 1442–1456. <https://doi.org/10.1093/pm/pnac029>
- Levade, T., Andrieu-Abadie, N., Ségui, B., Augé, N., Chatelut, M., Jaffrézou, J. P., & Salvayre, R. (1999). Sphingomyelin-degrading pathways in human cells role in cell signalling. *Chemistry and Physics of Lipids*, 102(1–2), 167–178. [https://doi.org/10.1016/s0009-3084\(99\)00085-7](https://doi.org/10.1016/s0009-3084(99)00085-7)
- Lim, K. G., Tonelli, F., Li, Z., Lu, X., Bittman, R., Pyne, S., & Pyne, N. J. (2011). FTY720 Analogues as sphingosine kinase 1 inhibitors: Enzyme inhibition kinetics, allostery, proteasomal degradation, and Actin rearrangement in MCF-7 breast cancer cells. *The Journal of Biological Chemistry*, 286(21), 18633–18640. <https://doi.org/10.1074/jbc.M111.220756>
- Lohner, K. (1996). Is the high propensity of ethanolamine plasmalogens to form non-lamellar lipid structures manifested in the properties of biomembranes? *Chemistry and Physics of Lipids*, 81(2), 167–184. [https://doi.org/10.1016/0009-3084\(96\)02580-7](https://doi.org/10.1016/0009-3084(96)02580-7)



- Magaquian, D., Delgado Ocaña, S., Perez, C., & Banchio, C. (2021). Phosphatidylcholine restores neuronal plasticity of neural stem cells under inflammatory stress. *Scientific Reports*, 11(1), 22891. <https://doi.org/10.1038/s41598-021-02361-5>
- Mandala, S., Hajdu, R., Bergstrom, J., Quackenbush, E., Xie, J., Milligan, J., Thornton, R., Shei, G. J., Card, D., Keohane, C., Rosenbach, M., Hale, J., Lynch, C. L., Rupprecht, K., Parsons, W., & Rosen, H. (2002). Alteration of lymphocyte trafficking by sphingosine-1-phosphate receptor agonists. *Science (New York, N.Y.)*, 296(5566), 346–349. <https://doi.org/10.1126/science.1070238>
- Matloubian, M., Lo, C. G., Cinamon, G., Lesneski, M. J., Xu, Y., Brinkmann, V., Allende, M. L., Proia, R. L., & Cyster, J. G. (2004). Lymphocyte egress from thymus and peripheral lymphoid organs is dependent on S1P receptor 1. *Nature*, 427(6972), 355–360. <https://doi.org/10.1038/nature02284>
- Mawatari, S., Ohara, S., Taniwaki, Y., Tsuboi, Y., Maruyama, T., & Fujino, T. (2020). Improvement of blood plasmalogens and clinical symptoms in Parkinson's disease by oral administration of Ether phospholipids: A preliminary report. *Parkinson's Disease*, 2020, 2671070. <https://doi.org/10.1155/2020/2671070>
- Messias, M. C. F., Mecatti, G. C., Priolli, D. G., & de Oliveira Carvalho, P. (2018). Plasmalogen lipids: Functional mechanism and their involvement in gastrointestinal cancer. *Lipids in Health and Disease*, 17(1), 41. <https://doi.org/10.1186/s12944-018-0685-9>
- Metzler, B., Gfeller, P., Wiczorek, G., Li, J., Nuesslein-Hildesheim, B., Katopodis, A., Mueller, M., & Brinkmann, V. (2008). Modulation of T cell homeostasis and alloreactivity under continuous FTY720 exposure. *International Immunology*, 20(5), 633–644. <https://doi.org/10.1093/intimm/dxn023>
- Mielke, M. M., Maetzler, W., Haughey, N. J., Bandaru, V. V., Savica, R., Deuschle, C., Gasser, T., Hauser, A. K., Gräber-Sultan, S., Schleicher, E., Berg, D., & Liepelt-Scarfone, I. (2013). Plasma ceramide and glucosylceramide metabolism is altered in sporadic Parkinson's disease and associated with cognitive impairment: A pilot study. *PLoS One*, 8(9), e73094. <https://doi.org/10.1371/journal.pone.0073094>
- Miguez, A., García-Díaz Barriga, G., Brito, V., Straccia, M., Giral, A., Ginés, S., Canals, J. M., & Alberch, J. (2015). Fingolimod (FTY720) enhances hippocampal synaptic plasticity and memory in Huntington's disease by preventing p75NTR up-regulation and astrocyte-mediated inflammation. *Human Molecular Genetics*, 24(17), 4958–4970. <https://doi.org/10.1093/hmg/ddv218>
- Miron, V. E., Schubart, A., & Antel, J. P. (2008). Central nervous system-directed effects of FTY720 (fingolimod). *Journal of the Neurological Sciences*, 274(1–2), 13–17. <https://doi.org/10.1016/j.jns.2008.06.031>
- Mohamed, A., Molendijk, J., & Hill, M. M. (2020). Lipidr: A software tool for data mining and analysis of Lipidomics datasets. *Journal of Proteome Research*, 19(7), 2890–2897. <https://doi.org/10.1021/acs.jproteome.0c00082>
- Molendijk, M. L., & de Kloet, E. R. (2019). Coping with the forced swim stressor: Current state-of-the-art. *Behavioural Brain Research*, 364, 1–10. <https://doi.org/10.1016/j.bbr.2019.02.005>
- Morris, R. G. M. (1981). Spatial localization does not require the presence of local cues. *Learning and Motivation*, 12, 239–260. [https://doi.org/10.1016/0023-9690\(81\)90020-5](https://doi.org/10.1016/0023-9690(81)90020-5)
- Moser, M. B., Moser, E. I., Forrester, E., Andersen, P., & Morris, R. G. (1995). Spatial learning with a minilab in the dorsal hippocampus. *Proceedings of the National Academy of Sciences of the United States of America*, 92(21), 9697–9701. <https://doi.org/10.1073/pnas.92.21.9697>
- Müller, C. P., Reichel, M., Mühle, C., Rhein, C., Gulbins, E., & Kornhuber, J. (2015). Brain membrane lipids in major depression and anxiety disorders. *Biochimica et Biophysica Acta*, 1851(8), 1052–1065. <https://doi.org/10.1016/j.bbali.2014.12.014>
- Mullershausen, F., Craveiro, L. M., Shin, Y., Cortes-Cros, M., Bassilana, F., Osinde, M., Wishart, W. L., Guerini, D., Thallmair, M., Schwab, M. E., Sivasankaran, R., Seuwen, K., & Dev, K. K. (2007). Phosphorylated FTY720 promotes astrocyte migration through sphingosine-1-phosphate receptors. *Journal of Neurochemistry*, 102(4), 1151–1161. <https://doi.org/10.1111/j.1471-4159.2007.04629.x>
- Myers, O. D., Sumner, S. J., Li, S., Barnes, S., & Du, X. (2017). Detailed investigation and comparison of the XCMS and MZmine 2 chromatogram construction and chromatographic peak detection methods for preprocessing mass spectrometry metabolomics data. *Analytical Chemistry*, 89(17), 8689–8695. <https://doi.org/10.1021/acs.analchem.7b01069>
- Nagahara, Y., Ikekita, M., & Shinomiya, T. (2000). Immunosuppressant FTY720 induces apoptosis by direct induction of permeability transition and release of cytochrome c from mitochondria. *Journal of Immunology (Baltimore, Md.: 1950)*, 165(6), 3250–3259. <https://doi.org/10.4049/jimmunol.165.6.3250>
- National Library of Medicine (U.S.). (2019). Fingolimod in treating patients with chemotherapy-induced neuropathy. Identifier NCT03943498. Retrieved 27 July 2023 from <https://classic.clinicaltrials.gov/ct2/show/NCT03943498?term=gilenya&draw=2>
- Nayak, D., Huo, Y., Kwang, W. X., Pushparaj, P. N., Kumar, S. D., Ling, E. A., & Dheen, S. T. (2010). Sphingosine kinase 1 regulates the expression of proinflammatory cytokines and nitric oxide in activated microglia. *Neuroscience*, 166(1), 132–144. <https://doi.org/10.1016/j.neuroscience.2009.12.020>
- Nazari, M., Keshavarz, S., Rafati, A., Namavar, M. R., & Haghani, M. (2016). Fingolimod (FTY720) improves hippocampal synaptic plasticity and memory deficit in rats following focal cerebral ischemia. *Brain Research Bulletin*, 124, 95–102. <https://doi.org/10.1016/j.brainresbu.2016.04.004>
- O'Brien, J. S., & Sampson, E. L. (1965). Lipid composition of the normal human brain: Gray matter, white matter, and myelin. *Journal of Lipid Research*, 6(4), 537–544.
- Oliveira, T. G., Chan, R. B., Tian, H., Laredo, M., Shui, G., Staniszewski, A., Zhang, H., Wang, L., Kim, T.-W., Duff, K. E., Wenk, M. R., Arancio, O., & Di Paolo, G. (2010). Phospholipase D2 ablation ameliorates Alzheimer's disease-linked synaptic dysfunction and cognitive deficits. *Journal of Neuroscience*, 30(49), 16419–16428. <https://doi.org/10.1523/JNEUROSCI.3317-10.2010>
- Olsen, A. S. B., & Færgeman, N. J. (2017). Sphingolipids: Membrane microdomains in brain development, function and neurological diseases. *Open Biology*, 7(5), 170069. <https://doi.org/10.1098/rsob.170069>
- Ong, W. Y., Herr, D. R., Farooqui, T., Ling, E. A., & Farooqui, A. A. (2015). Role of sphingomyelinases in neurological disorders. *Expert Opinion on Therapeutic Targets*, 19(12), 1725–1742. <https://doi.org/10.1517/14728222.2015.1071794>
- Oo, M. L., Thangada, S., Wu, M. T., Liu, C. H., Macdonald, T. L., Lynch, K. R., Lin, C. Y., & Hla, T. (2007). Immunosuppressive and anti-angiogenic sphingosine 1-phosphate receptor-1 agonists induce ubiquitinylation and proteasomal degradation of the receptor. *The Journal of Biological Chemistry*, 282(12), 9082–9089. <https://doi.org/10.1074/jbc.M610318200>
- Osinde, M., Mullershausen, F., & Dev, K. K. (2007). Phosphorylated FTY720 stimulates ERK phosphorylation in astrocytes via S1P receptors. *Neuropharmacology*, 52(5), 1210–1218. <https://doi.org/10.1016/j.neuropharm.2006.11.010>
- Oskolkova, O. V., Afonyushkin, T., Preinerstorfer, B., Bicker, W., von Schlieffen, E., Hainzl, E., Demyanets, S., Schabbauer, G., Lindner, W., Tselepis, A. D., Wojta, J., Binder, B. R., & Bochkov, V. N. (2010). Oxidized phospholipids are more potent antagonists of lipopolysaccharide than inducers of inflammation. *Journal of Immunology*, 185(12), 7706–7712. <https://doi.org/10.4049/jimmunol.0903594>
- O'Sullivan, C., & Dev, K. K. (2013). The structure and function of the S1P1 receptor. *Trends in Pharmacological Sciences*, 34(7), 401–412. <https://doi.org/10.1016/j.tips.2013.05.002>
- O'Sullivan, S., & Dev, K. K. (2017). Sphingosine-1-phosphate receptor therapies: Advances in clinical trials for CNS-related diseases.

- Neuropharmacology*, 113(Pt B), 597–607. <https://doi.org/10.1016/j.neuropharm.2016.11.006>
- O'Sullivan, S. A., O'Sullivan, C., Healy, L. M., Dev, K. K., & Sheridan, G. K. (2018). Sphingosine 1-phosphate receptors regulate TL4-induced CXCL5 release from astrocytes and microglia. *Journal of Neurochemistry*, 144(6), 736–747. <https://doi.org/10.1111/jnc.14313>
- Oyama, Y., Chikahisa, L., Kanemaru, K., Nakata, M., Noguchi, S., Nagano, T., Okazaki, E., & Hirata, A. (1998). Cytotoxic actions of FTY720, a novel immunosuppressant, on thymocytes and brain neurons dissociated from the rat. *Japanese Journal of Pharmacology*, 76(4), 377–385. <https://doi.org/10.1254/jjp.76.377>
- Park, M. H., Park, K. H., Choi, B. J., Han, W. H., Yoon, H. J., Jung, H. Y., Lee, J., Song, I. S., Lim, D. Y., Choi, M. K., Lee, Y. H., Park, C. M., Wang, M., Jo, J., Kim, H. J., Kim, S. H., Schuchman, E. H., Jin, H. K., & Bae, J. S. (2022). Discovery of a dual-action small molecule that improves neuropathological features of Alzheimer's disease mice. *Proceedings of the National Academy of Sciences of the United States of America*, 119(3), e2115082119. <https://doi.org/10.1073/pnas.2115082119>
- Payne, S. G., Oskeritzian, C. A., Griffiths, R., Subramanian, P., Barbour, S. E., Chalfant, C. E., Milstien, S., & Spiegel, S. (2007). The immunosuppressant drug FTY720 inhibits cytosolic phospholipase A2 independently of sphingosine-1-phosphate receptors. *Blood*, 109(3), 1077–1085. <https://doi.org/10.1182/blood-2006-03-011437>
- Petsas, N., De Giglio, L., González-Quintanilla, V., Giuliani, M., De Angelis, F., Tona, F., Carmellini, M., Mainero, C., Pozzilli, C., & Pantano, P. (2019). Functional connectivity changes after initial treatment with Fingolimod in multiple sclerosis. *Frontiers in Neurology*, 10, 153. <https://doi.org/10.3389/fneur.2019.00153>
- Pieragostino, D., D'Alessandro, M., di Iorio, M., Rossi, C., Zucchelli, M., Urbani, A., Di Ilio, C., Lugaresi, A., Sacchetta, P., & Del Boccio, P. (2015). An integrated metabolomics approach for the research of new cerebrospinal fluid biomarkers of multiple sclerosis. *Molecular BioSystems*, 11(6), 1563–1572. <https://doi.org/10.1039/c4mb00700j>
- Pluskal, T., Castillo, S., Villar-Briones, A., & Oresic, M. (2010). MZmine 2: Modular framework for processing, visualizing, and analyzing mass spectrometry-based molecular profile data. *BMC Bioinformatics*, 11, 395. <https://doi.org/10.1186/1471-2105-11-395>
- Porsolt, R. D., Le Pichon, M., & Jalfre, M. (1977). Depression: A new animal model sensitive to antidepressant treatments. *Nature*, 266(5604), 730–732. <https://doi.org/10.1038/266730a0>
- Postila, P. A., & Róg, T. (2020). A perspective: Active role of lipids in neurotransmitter dynamics. *Molecular Neurobiology*, 57(2), 910–925. <https://doi.org/10.1007/s12035-019-01775-7>
- Pothuizen, H. H., Zhang, W. N., Jongen-Rêlo, A. L., Feldon, J., & Yee, B. K. (2004). Dissociation of function between the dorsal and the ventral hippocampus in spatial learning abilities of the rat: A within-subject, within-task comparison of reference and working spatial memory. *The European Journal of Neuroscience*, 19(3), 705–712. <https://doi.org/10.1111/j.0953-816x.2004.03170.x>
- Puchkov, D., & Haucke, V. (2013). Greasing the synaptic vesicle cycle by membrane lipids. *Trends in Cell Biology*, 23(10), 493–503. <https://doi.org/10.1016/j.tcb.2013.05.002>
- Qin, C., Fan, W. H., Liu, Q., Shang, K., Murugan, M., Wu, L. J., Wang, W., & Tian, D. S. (2017). Fingolimod protects against ischemic white matter damage by modulating microglia toward M2 polarization via STAT3 pathway. *Stroke*, 48(12), 3336–3346. <https://doi.org/10.1161/STROKEAHA.117.018505>
- Que, X., Hung, M., Yeang, C., Gonen, A., Prohaska, T. A., Sun, X., Diehl, C., Määttä, A., Gaddis, D. E., Bowden, K., Pattison, J., MacDonald, J. G., Ylä-Herttuala, S., Mellon, P. L., Hedrick, C. C., Ley, K., Miller, Y. I., Glass, C. K., Peterson, K. L., ... Witztum, J. L. (2018). Oxidized phospholipids are proinflammatory and proatherogenic in hypercholesterolemic mice. *Nature*, 558(7709), 301–306. <https://doi.org/10.1038/s41586-018-0198-8>
- Raben, D. M., & Barber, C. N. (2017). Phosphatidic acid and neurotransmission. *Advances in Biological Regulation*, 63, 15–21. <https://doi.org/10.1016/j.jbior.2016.09.004>
- Reardon, S. (2019). Depression researchers rethink popular mouse swim tests. *Nature*, 571(7766), 456–457. <https://doi.org/10.1038/d41586-019-02133-2>
- Rog, T., & Koivuniemi, A. (2016). The biophysical properties of ethanolamine plasmalogens revealed by atomistic molecular dynamics simulations. *Biochimica et Biophysica Acta*, 1858(1), 97–103. <https://doi.org/10.1016/j.bbamem.2015.10.023>
- Roggeri, A., Schepers, M., Tiane, A., Rombaut, B., van Veggel, L., Hellings, N., Prickaerts, J., Pittaluga, A., & Vanmierlo, T. (2020). Sphingosine-1-phosphate receptor modulators and Oligodendroglial cells: Beyond immunomodulation. *International Journal of Molecular Sciences*, 21(20), 7537. <https://doi.org/10.3390/ijms21207537>
- Romero, L. O., Massey, A. E., Mata-Daboin, A. D., Sierra-Valdez, F. J., Chauhan, S. C., Cordero-Morales, J. F., & Vásquez, V. (2019). Dietary fatty acids fine-tune Piezo1 mechanical response. *Nature Communications*, 10(1), 1200. <https://doi.org/10.1038/s41467-019-09055-7>
- Rossi, S., Lo Giudice, T., De Chiara, V., Musella, A., Studer, V., Motta, C., Bernardi, G., Martino, G., Furlan, R., Martorana, A., & Centonze, D. (2012). Oral fingolimod rescues the functional deficits of synapses in experimental autoimmune encephalomyelitis. *British Journal of Pharmacology*, 165(4), 861–869. <https://doi.org/10.1111/j.1476-5381.2011.01579.x>
- Samuli Ollila, O. H., Róg, T., Karttunen, M., & Vattulainen, I. (2007). Role of sterol type on lateral pressure profiles of lipid membranes affecting membrane protein functionality: Comparison between cholesterol, desmosterol, 7-dehydrocholesterol and ketosterol. *Journal of Structural Biology*, 159(2), 311–323. <https://doi.org/10.1016/j.jsb.2007.01.012>
- Sanchez, T., Estrada-Hernandez, T., Paik, J. H., Wu, M. T., Venkataraman, K., Brinkmann, V., Claffey, K., & Hla, T. (2003). Phosphorylation and action of the immunomodulator FTY720 inhibits vascular endothelial cell growth factor-induced vascular permeability. *The Journal of Biological Chemistry*, 278(47), 47281–47290. <https://doi.org/10.1074/jbc.M306896200>
- Semple, B. D., Blomgren, K., Gimlin, K., Ferriero, D. M., & Noble-Haeusslein, L. J. (2013). Brain development in rodents and humans: Identifying benchmarks of maturation and vulnerability to injury across species. *Progress in Neurobiology*, 106–107, 1–16. <https://doi.org/10.1016/j.pneurobio.2013.04.001>
- Sharma, S., Mathur, A. G., Pradhan, S., Singh, D. B., & Gupta, S. (2011). Fingolimod (FTY720): First approved oral therapy for multiple sclerosis. *The Journal of Pharmacy and Pharmacology*, 2(1), 49–51. <https://doi.org/10.4103/0976-500X.77118>
- Sheridan, G. K., & Dev, K. K. (2012). S1P1 receptor subtype inhibits demyelination and regulates chemokine release in cerebellar slice cultures. *Glia*, 60(3), 382–392. <https://doi.org/10.1002/glia.22272>
- Sheridan, G. K., & Dev, K. K. (2014). Targeting S1P receptors in experimental autoimmune encephalomyelitis in mice improves early deficits in locomotor activity and increases ultrasonic vocalisations. *Scientific Reports*, 4, 5051. <https://doi.org/10.1038/srep05051>
- Slowik, A., Schmidt, T., Beyer, C., Amor, S., Clarner, T., & Kipp, M. (2015). The sphingosine 1-phosphate receptor agonist FTY720 is neuroprotective after cuprizone-induced CNS demyelination. *British Journal of Pharmacology*, 172(1), 80–92. <https://doi.org/10.1111/bph.12938>
- Solati, Z., Edel, A. L., Shang, Y., Karmin, O., & Ravandi, A. (2018). Oxidized phosphatidylcholines are produced in renal ischemia reperfusion injury. *PLoS One*, 13(4), e0195172. <https://doi.org/10.1371/journal.pone.0195172>
- Sonnino, S., & Prinetti, A. (2016). The role of sphingolipids in neuronal plasticity of the brain. *Journal of Neurochemistry*, 137(4), 485–488. <https://doi.org/10.1111/jnc.13589>



- Stessin, A. M., Banu, M. A., Clausi, M. G., Berry, N., Boockvar, J. A., & Ryu, S. (2017). FTY720/fingolimod, an oral S1PR modulator, mitigates radiation induced cognitive deficits. *Neuroscience Letters*, 658, 1–5. <https://doi.org/10.1016/j.neulet.2017.08.025>
- Sun, Y., Hong, F., Zhang, L., & Feng, L. (2016). The sphingosine-1-phosphate analogue, FTY-720, promotes the proliferation of embryonic neural stem cells, enhances hippocampal neurogenesis and learning and memory abilities in adult mice. *British Journal of Pharmacology*, 173(18), 2793–2807. <https://doi.org/10.1111/bph.13557>
- Swain, J., Mohapatra, M., Borkar, S. R., Aidhen, I. S., & Mishra, A. K. (2013). Study of aqueous phase aggregation of FTY720 (fingolimod hydrochloride) and its effect on DMPC liposomes using fluorescent molecular probes. *Physical Chemistry Chemical Physics (PCCP)*, 15(41), 17962–17970. <https://doi.org/10.1039/c3cp53148a>
- Szlasa, W., Zendran, I., Zalesińska, A., Tarek, M., & Kulbacka, J. (2020). Lipid composition of the cancer cell membrane. *Journal of Bioenergetics and Biomembranes*, 52(5), 321–342. <https://doi.org/10.1007/s10863-020-09846-4>
- Takasaki, T., Hagihara, K., Satoh, R., & Sugiura, R. (2018). More than just an immunosuppressant: The emerging role of FTY720 as a novel inducer of ROS and Apoptosis. *Oxidative Medicine and Cellular Longevity*, 2018, 4397159. <https://doi.org/10.1155/2018/4397159>
- Tanguy, E., Wang, Q., Moine, H., & Vitale, N. (2019). Phosphatidic acid: From pleiotropic functions to neuronal pathology. *Frontiers in Cellular Neuroscience*, 13, 2. <https://doi.org/10.3389/fncel.2019.00002>
- Tham, C. S., Lin, F. F., Rao, T. S., Yu, N., & Webb, M. (2003). Microglial activation state and lysophospholipid acid receptor expression. *International Journal of Developmental Neuroscience: The Official Journal of the International Society for Developmental Neuroscience*, 21(8), 431–443. <https://doi.org/10.1016/j.ijdevneu.2003.09.003>
- Tyanova, S., Temu, T., Sinitcyn, P., Carlson, A., Hein, M. Y., Geiger, T., Mann, M., & Cox, J. (2016). The Perseus computational platform for comprehensive analysis of (prote)omics data. *Nature Methods*, 13(9), 731–740. <https://doi.org/10.1038/nmeth.3901>
- Tzekov, R., Dawson, C., Orlando, M., Mouzon, B., Reed, J., Evans, J., Crynen, G., Mullan, M., & Crawford, F. (2016). Sub-chronic neuropathological and biochemical changes in mouse visual system after repetitive mild traumatic brain injury. *PLoS One*, 11(4), e0153608. <https://doi.org/10.1371/journal.pone.0153608>
- Udagawa, J., & Hino, K. (2022). Plasmalogen in the brain: Effects on cognitive functions and behaviors attributable to its properties. *Brain Research Bulletin*, 188, 197–202. <https://doi.org/10.1016/j.brainresbull.2022.08.008>
- van Doorn, R., Nijland, P. G., Dekker, N., Witte, M. E., Lopes-Pinheiro, M. A., van het Hof, B., Kooij, G., Reijkerker, A., Dijkstra, C., van der Valk, P., van Horssen, J., & de Vries, H. E. (2012). Fingolimod attenuates ceramide-induced blood-brain barrier dysfunction in multiple sclerosis by targeting reactive astrocytes. *Acta Neuropathologica*, 124(3), 397–410. <https://doi.org/10.1007/s00401-012-1014-4>
- Vásquez, V., Krieg, M., Lockhead, D., & Goodman, M. B. (2014). Phospholipids that contain polyunsaturated fatty acids enhance neuronal cell mechanics and touch sensation. *Cell Reports*, 6(1), 70–80. <https://doi.org/10.1016/j.celrep.2013.12.012>
- Velasco-Estevez, M., Gadalla, K. K. E., Liñan-Barba, N., Cobb, S., Dev, K. K., & Sheridan, G. K. (2020). Inhibition of Piezo1 attenuates demyelination in the central nervous system. *Glia*, 68(2), 356–375. <https://doi.org/10.1002/glia.23722>
- Vidal-Martinez, G., Najera, K., Miranda, J. D., Gil-Tommee, C., Yang, B., Vargas-Medrano, J., Diaz-Pacheco, V., & Perez, R. G. (2019). FTY720 improves behavior, increases brain derived neurotrophic factor levels and reduces α -Synuclein pathology in parkinsonian GM2+/- mice. *Neuroscience*, 411, 1–10. <https://doi.org/10.1016/j.neuroscience.2019.05.029>
- Wang, G., Kim, R. Y., Imhof, I., Honbo, N., Luk, F. S., Li, K., Kumar, N., Zhu, B. Q., Eberlé, D., Ching, D., Karliner, J. S., & Raffai, R. L. (2014). The immunosuppressant FTY720 prolongs survival in a mouse model of diet-induced coronary atherosclerosis and myocardial infarction. *Journal of Cardiovascular Pharmacology*, 63(2), 132–143. <https://doi.org/10.1097/FJC.0000000000000031>
- Watson, R. E., Desesso, J. M., Hurtt, M. E., & Cappon, G. D. (2006). Postnatal growth and morphological development of the brain: A species comparison. *Birth Defects Research. Part B, Developmental and Reproductive Toxicology*, 77(5), 471–484. <https://doi.org/10.1002/bdrb.20090>
- Wei, S. H., Rosen, H., Matheu, M. P., Sanna, M. G., Wang, S. K., Jo, E., Wong, C. H., Parker, I., & Cahalan, M. D. (2005). Sphingosine 1-phosphate type 1 receptor agonism inhibits transendothelial migration of medullary T cells to lymphatic sinuses. *Nature Immunology*, 6(12), 1228–1235. <https://doi.org/10.1038/ni1269>
- Woods, A. S., & Jackson, S. N. (2006). Brain tissue lipidomics: Direct probing using matrix-assisted laser desorption/ionization mass spectrometry. *The AAPS Journal*, 8(2), E391–E395. <https://doi.org/10.1007/BF02854910>
- Wu, C., Leong, S. Y., Moore, C. S., Cui, Q. L., Gris, P., Bernier, L. P., Johnson, T. A., Séguéla, P., Kennedy, T. E., Bar-Or, A., & Antel, J. P. (2013). Dual effects of daily FTY720 on human astrocytes in vitro: Relevance for neuroinflammation. *Journal of Neuroinflammation*, 10, 41. <https://doi.org/10.1186/1742-2094-10-41>
- Xue, J., Guijas, C., Benton, H. P., Warth, B., & Siuzdak, G. (2020). METLIN MS2 molecular standards database: A broad chemical and biological resource. *Nature Methods*, 17(10), 953–954. <https://doi.org/10.1038/s41592-020-0942-5>
- Yang, X., Sheng, W., Sun, G. Y., & Lee, J. C. (2011). Effects of fatty acid unsaturation numbers on membrane fluidity and α -secretase-dependent amyloid precursor protein processing. *Neurochemistry International*, 58(3), 321–329. <https://doi.org/10.1016/j.neuint.2010.12.004>
- Yang, X., Sun, G. Y., Eckert, G. P., & Lee, J. C. (2014). Cellular membrane fluidity in amyloid precursor protein processing. *Molecular Neurobiology*, 50(1), 119–129. <https://doi.org/10.1007/s12035-014-8652-6>
- Yankelevitch-Yahav, R., Franko, M., Huly, A., & Doron, R. (2015). The forced swim test as a model of depressive-like behavior. *Journal of Visualized Experiments: JoVE*, 97, 52587. <https://doi.org/10.3791/52587>
- Yazdi, A., Baharvand, H., & Javan, M. (2015). Enhanced remyelination following lysocleithin-induced demyelination in mice under treatment with fingolimod (FTY720). *Neuroscience*, 311, 34–44. <https://doi.org/10.1016/j.neuroscience.2015.10.013>
- Young, M. M., Bui, V., Chen, C., & Wang, H. G. (2019). FTY720 induces non-canonical phosphatidylserine externalization and cell death in acute myeloid leukemia. *Cell Death & Disease*, 10(11), 847. <https://doi.org/10.1038/s41419-019-2080-5>
- Yu, X., Qi, X., Wei, L., Zhao, L., Deng, W., Guo, W., Wang, Q., Ma, X., Hu, X., Ni, P., & Li, T. (2023). Fingolimod ameliorates schizophrenia-like cognitive impairments induced by phencyclidine in male rats. *British Journal of Pharmacology*, 180(2), 161–173. <https://doi.org/10.1111/bph.15954>
- Zemann, B., Kinzel, B., Müller, M., Reuschel, R., Mechtcheriakova, D., Urtz, N., Bornancin, F., Baumruker, T., & Billich, A. (2006). Sphingosine kinase type 2 is essential for lymphopenia induced by the immunomodulatory drug FTY720. *Blood*, 107(4), 1454–1458. <https://doi.org/10.1182/blood-2005-07-2628>
- Zhang, M., Hu, Y., Zhang, J., & Zhang, J. (2021). FTY720 prevents spatial memory impairment in a rat model of chronic cerebral Hypoperfusion via a SIRT3-independent pathway. *Frontiers in Aging Neuroscience*, 12, 593364. <https://doi.org/10.3389/fnagi.2020.593364>
- Zhao, Y., Shi, D., Cao, K., Wu, F., Zhu, X., Wen, S., You, Q., Zhang, K., Liu, L., & Zhou, H. (2018). Fingolimod targets cerebral endothelial activation to block leukocyte recruitment in the central nervous system. *Journal of Leukocyte Biology*, 103(1), 107–118. <https://doi.org/10.1002/JLB.3A0717-287R>
- Zhou, M. M., Xue, Y., Sun, S. H., Wen, M., Li, Z. J., Xu, J., Wang, J. F., Yanagita, T., Wang, Y. M., & Xue, C. H. (2016). Effects of different fatty acids composition of phosphatidylcholine on brain function of



dementia mice induced by scopolamine. *Lipids in Health and Disease*, 15(1), 135. <https://doi.org/10.1186/s12944-016-0305-5>

Zoeller, R. A., Grazia, T. J., LaCamera, P., Park, J., Gaposchkin, D. P., & Farber, H. W. (2002). Increasing plasmalogen levels protects human endothelial cells during hypoxia. *American Journal of Physiology. Heart and Circulatory Physiology*, 283(2), H671–H679. <https://doi.org/10.1152/ajpheart.00524.2001>

SUPPORTING INFORMATION

Additional supporting information can be found online in the Supporting Information section at the end of this article.

How to cite this article: Magalhães, D. M., Stewart, N. A., Mampay, M., Rolle, S. O., Hall, C. M., Moendarbary, E., Flint, M. S., Sebastião, A. M., Valente, C. A., Dymond, M. K., & Sheridan, G. K. (2024). The sphingosine 1-phosphate analogue, FTY720, modulates the lipidomic signature of the mouse hippocampus. *Journal of Neurochemistry*, 00, 1–30. <https://doi.org/10.1111/jnc.16073>